Ref. Ares(2015)5473147 - 30/11/2015

FATIMA

FArming Tools for external nutrient Inputs and water MAnagement

D2.2.2: Methodology manual for EO-based crop water requirements forecast

WP2.2 EO for monitoring plant status and yield

Guido D'Urso, Carlo De Michele (Ariespace)

with inputs from Agricultural University of Athens; Nikolaos Spyropoulos, SIGMA Geotechnologie, Alfonso Calera, UCLM

European Commission

Horizon 2020
European Union funding
for Research & Innovation

This project has received funding from the European Union's Horizon 2020 research and innovation programme under grant agreement No 633945.

Document Information

Grant Agreement Number	633945	**Acronym**	FATIMA	
Full Title of Project	Farming Tools for external nutrient inputs and water Management			
Horizon 2020 Call	SFS-02a-2014: External nutrient inputs (Research and innovation Action)			
Start Date	1 March 2015	**Duration**	36 months	
Project website	www.fatima-h2020.eu			
Document URL	(insert URL if document is publicly available online)			
REA Project Officer	Aneta RYNIAK			
Project Coordinator	Anna Osann			
Deliverable	D2.2.1 Methodology manual for EO-based crop water requirements forecast			
Work Package	WP2.2 – EO for monitoring plant status and yield			
Date of Delivery	**Contractual**	30 November 2015	**Actual**	30 November 2015
Nature	R - Report	**Dissemination Level**	PU	
Lead Beneficiary	04_ARIESPACE			
Lead Author	Guido D'Urso (ARIESPACE)	**Email**	durso@unina,it	
Contributions from				
internal Reviewer 1	Ali Gul (EA-TEK)			
Internal Reviewer 2	Nicos Spyropulos (SIGMA)			
Objective of document	To describe the methodology for EO-based forecast of crop water requirements for the next week and irrigation water requirements from EO driven soil water balance .			
Readership/Distribution	All FATIMA Regional Teams; All WP leaders and other FATIMA team members; European Commission / REA			
Keywords	Evapotranspiration, weather forecasting, remote sensing, monitoring data, crop water balance			

Document History

Version	Issue Date	Stage	Changes	Contributor
1.0	3/8/2015	draft	Main structure and contents	G. D'Urso
1.1	19/9/2015	draft	Integration of contents and harmonis.	C. De Michele
2.0	19/11/2015	draft	Integration of contents and Revision	C. De Michele. A.Calera, N.Spyropoulos
2.1	24/11/2015	draft	Integration of contents and Revision	C. De Michele.
2.2	30/11/2015	Final draft	Text revised for reviewers	C. De Michele

Disclaimer

Any dissemination of results reflects only the authors' view and the European Commission is not responsible for any use that may be made of the information it contains.

Copyright

© FATIMA Consortium, 2015
This deliverable contains original unpublished work except where clearly indicated otherwise. Acknowledgement of previously published material and of the work of others has been made through appropriate citation, quotation or both. Reproduction is authorised provided the source is acknowledged. Creative Commons licensing level

Executive summary

The EO methodology for mapping crop water requirements in a pixel by pixel basis is mature and operational by using FAO56 and soil water balance model, in combination with biophysical crop parameters and meteorological data. Consolidation of this approach will be the first step to do, including the implementation of algorithms for separating soil evaporation and canopy transpiration. The improved spectral resolution of new generation of sensors will be exploited to enhance existing methodologies.

The forward step is to produce crop water requirements predictions for the next week (maps), which is a very practical product for users in addition to the estimates for the past week. Numerical weather prediction model outputs can be efficiently applied for retrieving reliable forecasts of the reference evapotranspiration, needed for optimization of the irrigation scheduling at farm level. To this end, distributed short term forecasting of relevant meteorological data (from global or high-resolution limited area numerical weather prediction models) can be used as input in the above mentioned crop evapotranspiration models. Having the knowledge of crop water requirements, irrigation can be supplied either to satisfy full requirements, or either to manage a deficit controlled irrigation. Soil moisture measurements will provide all the adequate data to verify, through the soil water balance, the quality of the products.

Table of Contents

Executive summary 3
1 Introduction 6
2 Operative Methodologies to Determine Crop Water Requirements from Earth Observation Data 6
2.1 Crop Water requirement and evapotranspiration concepts 6
2.1.1 Reference evapotranspiration ET_0 6
2.1.1.1 Daily reference evapotranspiration ET_0 computation 7
2.1.2 Crop evapotranspiration under standard conditions: potential crop evapotranspiration (ET_p) 8
2.1.3 Crop Water requirement 8
2.2 K_c-NDVI approach 9
2.2.1 K_c-NDVI approach set for Spain 11
2.2.2 K_c-NDVI approach set in Greek site by Landsat 8 13
2.2.3 K_C- RedEdge NDVI approach set in Greek site using WW2 images 14
2.3 ET_p direct calculation, based on the application of the Penman- Monteith equation 14
2.3.1 Description of the processing chain and data used 15
3 Methodology for EO-based crop and soil water balance 19
3.1 Background on water balance models 19
3.1.1 Static modelling approach (bucket concept) 20
3.1.2 Dynamic modelling approach (Richards equation) 20
4 Application of numerical weather prediction (NWP) models for forecasting crop evapotranspiration . 24
4.1 Weather forecasts for agriculture 24
4.2 Numerical weather prediction (NWP) models 24
4.3 Domain Coverage: General Circulation Models (GCM) and Limited Area Models (LAM) 26
4.3.1 Ensemble forecasting systems 29
4.4 Operational weather prediction models in Europe: The COSMO-Model 30
4.5 COSMO-LEPS (Limited Area Ensemble Prediction System) 31
4.6 HIRLAM (HIgh Resolution Limited Area Model) 32
4.7 Fatima-WRF-Meteo-Tool 33
4.8 Forecasting reference evapotranspiration with NWP model 33
4.8.1 Example of Forecasting reference evapotranspiration (ET0) 34
4.8.1.1 Comparison 34
4.9 Forecasting potential evapotranspiration ET_p using numerical weather prediction (NWP) and assimilating LAI from remote sensing data in crop model with Ensemble Kalman Filter. 36
4.9.1 Example of Forecasting Potential evapotranspiration (ETp) 38
References 40

List of Tables

Table 3.1 - A selection of various categories of deterministic models for the unsaturated zone that are suitable to describe irrigation and drainage processes (the models and corresponding authors are listed in chronological sequence) 20
Table 4.1 - advantages of the WRF model in comparison with the current available solutions 25
Table 4.2 - Global Model Providers 27
Table 4.3 - Most Limited Area Models 28
Table 4.4 - Limited Area Ensemble Models 29
Table 4.5 - Details of the coarse applications of all COSMO partners 30

List of Figures

Figure 2.1 - Temporal evolution of crop coefficient Kcb and of NDVI in a maize field during 2001 growing season. Kcb has been estimated from fractional vegetation cover using FAO methodology. 10
Figure 2.2 - Figure Field observations of Kcb and of NDVI versus DoY for a maize field. 11
Figure 2.3 - The Kc classified values distribution, for the Landsat-8 images on June 14th and August 1st 2015, respectively 13
Figure 2.4 - The role of Kc in the estimation of Evapotranspiration 14
Figure 2.5 - Flow-chart of the processing chain after image delivery. [22] 16
Figure 2.6 - Comparison of evapotranspiration ETp, calculated for five years of summer daily meteo data by using Eq. (2.15), Sele plain, Campania, Italy, for hc= 0.4 and 1 m and twodifferent LAI values. [22] 18
Figure 3.1 - Root water uptake function α(h); the critical values of pressure head h are crop-dependent; h3 has two different values respectively for high and low potential transpiration rate 21
Figure 3.2 - Example of SWAP output concerning the vertical distribution of pressure head h (left) and soil water content θ (right) in a three-layered profile with the ground water table at 2 m depth at time t. Critical values of pressure head and soil water deficit in the root zone are used to determine irrigation schedules and amounts 22
Figure 4.1 - Operational domains of the coarse applications of all COSMO partners 31
Figure 4.2 - Operational domains of the coarse applications of COSMO-LEPS 32
Figure 4.3 - Study area, meteorological stations (red squares) and COSMO-LEPS grid points (blue circles) .. 34
Figure 4.4 - Comparison between the predicted daily ET0 computed by Penman-Monteith (ET0 - PM) Hargreaves-Samani (ET0 - HS) and Priestley-Taylor (ET0 - PT) with observed daily ET0 computed by Penman-Monteith at AWS no. 11 (i.e. Rocca D'Evandro) for 1 day lead time. The predicted values are the median of the ensemble forecasts and the dotted lines refer to the 10th and 90th percentiles. 35
Figure 4.5 - Comparison between the predicted daily ET0 computed by Penman-Monteith (ET0 - PM) Hargreaves-Samani (ET0 - HS) and Priestley-Taylor (ET0 - PT) with observed daily ET0 computed by Penman-Monteith at AWS no. 11 (i.e. Rocca D'Evandro) for 5 days lead time. The predicted values are the median of the ensemble forecasts and the dotted lines refer to the 10th and 90th percentiles. 36
Figure 4.6 - Schema of A simplified crop growth model 37

1 Introduction

In a high level approach, this document is proposing a simplified version of a manual which can be used by remote sensing professionals that operate in the field or agronomists that they are using a remote sensing tool coupled with numerical weather predictions models, to manage and consult certain number of farmers or even new farmers with technology background that they are willing to personally integrate Earth Observation (EO) data into their daily agricultural practices and agri-business. It is also a trial to be incorporated into FATIMA farmer training system.

The fundamental idea of this manual stems from the hypothesis that it is possible to perform a real time and seasonal estimation of water needs of crops of agricultural farms by cross correlating high spatial, spectral and temporal resolution of satellite data, acquired at well-defined time intervals of the phenological cycle of crops with ground-truth information simultaneously applied during the image acquisitions, thus creating a cost-effective methodology to reduce the inputs interpreted as irrigation at farm level.

2 Operative Methodologies to Determine Crop Water Requirements from Earth Observation Data

2.1 Crop Water requirement and evapotranspiration concepts

2.1.1 Reference evapotranspiration ET_0

The evapotranspiration rate from a reference surface, not short of water, is called the reference crop evapotranspiration or reference evapotranspiration and is denoted as ET_0. The reference surface is a hypothetical grass reference crop with specific characteristics. The use of other denominations such as potential ET is strongly discouraged due to ambiguities in their definitions.

The concept of the reference evapotranspiration was introduced to study the evaporative demand of the atmosphere independently of crop type, crop development and management practices. As water is abundantly available at the reference surface, ET is independent from limiting soil factors. Relating ET to a specific surface provides a reference to which ET from other surfaces can be related. It obviates the need to define a separate ET level for each crop and stage of growth. ET_0 values measured or calculated at different locations or in different seasons are comparable as they refer to the ET from the same reference surface.

The only factors affecting ET_0 are climatic parameters. Consequently, ET_0 is a climatic parameter and is computed from weather data. ET_0 expresses the evaporating power of the atmosphere at a specific location and time of the year and does not consider the crop characteristics and soil factors. The FAO Penman-Monteith method is recommended as the sole method for determining ET_0. The method has been selected because it closely approximates grass ET_0 at the location evaluated, is physically based, and explicitly incorporates both physiological and aerodynamic parameters. Moreover, procedures have been developed for estimating missing climatic parameters.

2.1.1.1 Daily reference evapotranspiration ET_0 computation

The Penman-Monteith equation combines meteorological and data referring to the reference grass for estimating ET_0. The minimum set of meteorological data is represented by: 2m air temperature and 2m relative humidity, short wavesolar radiation, 2m wind speed; in addition, the reference crop is characterized by four parameters: surface albedo (r), Leaf Area Index (LAI), canopy height (h_c) and leaf resistance; this latter parameter, for well-water crops, can be taken as a constant value (100 s/m). The P-M equation has been considered to be one of the most accurate approaches for estimating ET for crops and hence it has been adopted in the context of FAO procedure described in the Paper no.56 [1]. In the FAO procedure, the reference surface is an ideal crop, characterized by an albedo of 0.23, LAI=2.88 and h_c= 0.12-0.15 m. It corresponds likely to a grass surface uniformly covering the soil surface and adequately furnished with water. With these values, the P-M is written in the following form, representing the "FAO Penman-Monteith" equation for reference evapotranspiration ET_{0-PM} :

$$ET_{0-PM} = \frac{0.408\Delta(R_n - G) + \gamma \frac{900}{T+273} u_2 (e_s - e_a)}{\Delta + \gamma(1 + 0.34u_2)} \qquad [\text{mm/day}] \tag{2.1}$$

where R_n is the net radiation at the crop surface [$MJm^{-2}day^{-1}$], G is the soil heat flux density [$MJm^{-2}day^{-1}$], T is the daily mean air temperature at 2 m height [°C], u_2 is the wind speed at 2 m height [ms^{-1}], e_s is the saturation vapour pressure [kPa], e_a is the actual vapour pressure [kPa], Δ is the slope of the vapour pressure curve [$kPa°C^{-1}$] and γ is the psychometric constant [$kPa°C^{-1}$]. The daily mean air temperature is computed as mean between daily maximum (T_{max} [°C]) and minimum (T_{min} [°C]) temperatures while the actual vapour pressure is derived from the daily mean relative humidity RH [%] as suggested by [1].

Alternatively, the Hargreaves and Samani method [2] is the one suggested in the FAO guidelines [1] for estimating ET_0, when only temperature data are available.

The Hargreaves and Samani formula is given as:

$$ET_{0-HS} = K_{HS}(T + 17.8)\sqrt{T_{max} - T_{min}}(0.408R_a) \tag{2.2}$$

where ET_{0-HS} is the daily reference evapotranspiration in [$mmday^{-1}$], R_a is the extraterrestrial solar radiation [$MJm^{-2}day^{-1}$], T_{max} and T_{min} are the daily maximum and minimum 2m temperature [°C], respectively, K_{HS} is an empirical coefficient, assumed to be equal to 0.0023 as suggested by [1]. The formula only needs temperature data, since the extraterrestrial radiation is only a function of latitude and time of the year. However, its utilization for time-steps smaller than 10-15 days should be avoided.

Finally, the Priestley and Taylor [3] method can be considered:

$$ET_{0-PT} = \alpha \frac{\Delta(R_n - G)0.408}{\Delta + \gamma} + \beta$$

(2.3)

where $ET_{0\text{-}PT}$ is the daily reference evapotranspiration in [mmday^{-1}], α and β are empirical coefficients, assumed to be equal to 1.26 and 0, respectively, as found by the authors and theoretically explained by [4]. ET_{0-PT} mainly depends on net solar radiation, but 2m temperature data are still needed for computing R_n [1].

2.1.2 Crop evapotranspiration under standard conditions: potential crop evapotranspiration (ET_p)

The crop evapotranspiration under standard conditions, denoted as ET_p, is the evapotranspiration from disease-free, well-fertilized crops, grown in large fields, under optimum soil water conditions, and achieving full production under the given climatic conditions. In the original P-M equation, this condition implies a minimum for the leaf resistance, which can be considered as a constant for most crops. Experimentally determined ratios of ET_p/ET_0, called crop coefficients (K_c), are used to relate ET_p to ET_0

$$ET_P = K_c\, ET_0.$$

(2.4)

Moreover, the crop coefficient approach, as proposed by [5] and adopted within the FAO procedure, splits K_c into two separate coefficients, one for crop transpiration (K_{cb}, basal crop coefficient) and one for soil evaporation (K_e), which describes the evaporation component of *ET* :

$$ET_P = (K_{cb}+K_e)\, ET_0.$$

(2.5)

2.1.3 Crop Water requirement

The standard approach proposed by [1] for calculating crop water requirements (CWR) can be adapted to remote sensing data. Irrigation water requirements (CWR) are commonly calculated as follows:

$$CWR = ET_p - P_n$$

(2.6)

where ET_P (mm) is the crop evapotranspiration under standard conditions i.e. crops grown in large fields under excellent agronomic and soil water conditions; P_n, is effective precipitation depending on canopy development described by means of the Leaf Area Index LAI, and the fractional vegetation cover f_{cover}, accordingly to [6]:

$$P_n = P - aLAI\left(1 - \frac{1}{1 + \frac{f\text{cover} \cdot P}{aLAI}}\right) \quad (2.7)$$

with P (cm•d^{-1}), and a (cm•d^{-1}), being an empirical parameter representing the crop saturation per unit foliage area (~0.28 for most crops) and f_{cover} is the fractional vegetation cover derived from LAI by using a polynomial empirical expression, where coefficients are determined from field measurements and are valid for a wide range of crops (LAI≤ 5 m^2•m^{-2}).

The evaluation of potential evapotranspiration based on Earth Observation (E.O.) data for the operational assessment of crop water requirements is generally made by using the following procedures:

1. the approach based on the crop coefficient concept K_c, establishing a direct correspondence between K_c and reflectance measurements;
2. the direct calculation, "one-step" approach, based on the application of the Penman- Monteith equation with appropriate values of canopy variable such as crop height, surface albedo and Leaf Area Index (*LAI*).

2.2 K_c-NDVI approach

The estimation of potential crop evapotranspiration ET_p represents the basic information for the evaluation of crop water requirements. A widely used method to compute ET_p is based on the so-called "crop coefficient" K_c, defined as the ratio of total evapotranspiration by reference evapotranspiration ET_0. As confirmed by recent standard procedures of F.A.O., under given climatic conditions, the value of crop coefficient is related to canopy variables representing the crop growth stage, such as canopy height, fractional vegetation cover and Leaf Area Index. Considering that these canopy variables influence the spectral response of vegetated surfaces, a direct correspondence between K_c and reflectance measurements can be established. K_c is calculated by using reflectance-based estimates of canopy variables.

$$NDVI = \frac{\rho_{NIR} - \rho_R}{\rho_{NIR} + \rho_R} \quad (2.8)$$

The ability of NDVI to describe canopy biophysical variables i.e. fractional vegetation cover, fraction of absorbed photosynthetically active radiation, primary production, Leaf Area Index, basal crop coefficient parameter has been shown as follows:

1. *NDVI* is related linearly with fractional vegetation cover [**¡Error! No se encuentra el origen de la referencia.**, **¡Error! No se encuentra el origen de la referencia.**];
2. *NDVI* is related linearly with the fraction of absorbed photosynthetically active radiation (fAPAR) [**¡Error! No se encuentra el origen de la referencia.**];
3. *NDVI* is related with primary production (dry biomass) by means of Light Use Efficiency (*LUE*) models [**¡Error! No se encuentra el origen de la referencia.**, **¡Error! No se encuentra el origen de la referencia.**]; It establishes a relationship between *NDVI* and crop growth rate (*CGR*) can be established, thus in agreement with the idea that *NDVI* is an estimator of the canopy

photosynthetic power. This way, the vegetation index can be legitimately used to provide an estimate of growth rate.

4. *NDVI* is related exponentially with Leaf Area Index (*LAI*) [7]; is well known that *NDVI* begins to saturate for a value of *LAI* equal to 3 reaching a plateau for *LAI*>3.

Arguments pointed out in 3 and 4 may appear contradictory, due to the usual reasoning that relates higher *LAI* with higher evapotranspiration. However, in [8] it is stated that "the evidence seems conclusive that transpiration in most mesophytic crop plants and other mesophytic vegetation well supplied with water increases with leaf area to a *LAI* of about three". Accounting the *LAI* saturation in the relation with evapotranspiration has lead to the concept of active *LAI* in the [1].

The procedure to estimate K_{cb} is based in the knowledge of the fractional vegetation cover f_c; as such, the empirical relationship between *NDVI* and K_{cb} has been shown by many authors (Figure 2.1) [9], [10]. Despite the limitations due to variability associated with canopy structure, background soil, and calibration uncertainties, the *NDVI* can be used advantageously to estimate crop water requirements [11] in accounting its relationship with K_{cb}. A linear correlation between K_{cb} and *NDVI* has been explored also by other researchers [12] [13]. In order to minimize the presence of soil background, other vegetation indices have been used to compute K_{cb} [14]. This provides a particularly useful tool for satellite images where soil brightness and color can vary.

Intensive experimental campaigns were conducted at the main research facilities of the University of Castilla-La Mancha and the ITAP, in Las Tiesas (39º03'30''N; 2º05'24''W), within the Barrax pilot zone. The research field has a permanent lysimeter station, and a monitoring protocol adherent to FAO 56 specifications has been adopted [15]. In coincidence with field radiometric acquisitions, measurements of biomass (kg m^{-2}), *LAI* and f_c have also been carried out to describe the phenology of crops.

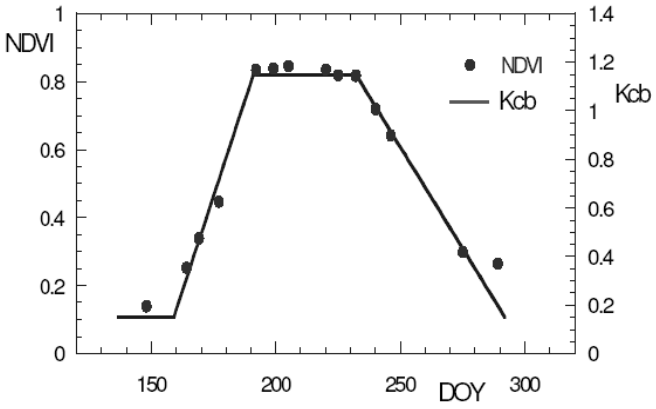

Figure 2.1 - Temporal evolution of crop coefficient Kcb and of NDVI in a maize field during 2001 growing season. Kcb has been estimated from fractional vegetation cover using FAO methodology.

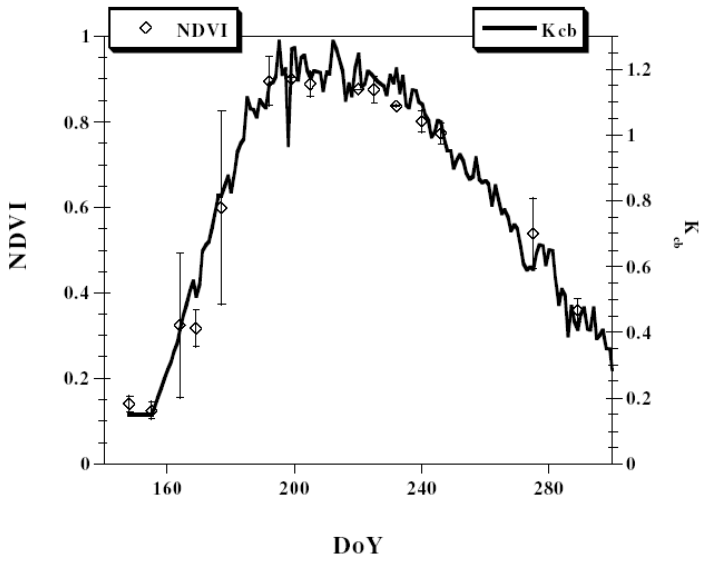

Figure 2.2 - Figure Field observations of Kcb and of NDVI versus DoY for a maize field.

By the knowledge of crop stages, K_{cb} values were estimated and corrected to take into account the effect of varying relative humidity and wind velocity from standard conditions (RH=40%, v = 2 ms^{-1}). Reflectance in red and near infrared to compute *NDVI* was obtained by integrating spectral reflectance in the range of 0.63-0.69 and 0.76-0.90 nm. The plot represented in Figure 2.2 gives an examples of results for a maize field; *NDVI* reaches its maximum value when crop reaches also full effective vegetation cover in coincidence to maximum of K_{cb}, thus confirming past researches. Linear regression analysis confirmed the existence of highly significant relationships between K_{cb} and vegetation indexes such as *NDVI*, *SAVI* and *PVI*.

2.2.1 K_c-NDVI approach set for Spain

A methodology has been set-up for the practical implementation of these research studies to operative applications based on E.O. data i.e. TM broadband data. The methodology has been tested during the 2003 pilot campaign in Barrax (Spain) for the following crops: barley, wheat, maize, opium plant, sugar beet, alfalfa, pea, potato, onion and garlic. Subsequent campaigns have been carried out on vineyards and natural vegetation [16][17] using ETM+ sensor and ground radiometry.

Accordingly these papers, and after an extensive review of published relationships about K_{cb}-NDVI, a linear relationship is adopted such as is expressed in eq. *(2.9)*.

$$K_{cb} = 1.44\ NDVI - 0.1 \quad (2.9)$$

Where:

- K_{cb} "spectral" basal crop coefficient [0.15 – 1.15],
- NDVI, calculated from surface reflectances on TM and ETM+ bands. [Typical range values: bare soil 0.12-0.16; maximum NDVI value for very dense green vegetation, 0.91]

The soil evaporation part in Eq. (2.5) needs to be accounted for the estimation of K_c. As is known, K_e, is related with bare soil fraction, and is strongly dependent on the wetting state of bare soil fraction, because the evaporative power of soil changes strongly if the soil is wetted or if the soil is dry. Irrigation system (gravity, sprinkler, drip, etc) and irrigation frequency, coupled with type and stage of crop, are the factors that determine the time of different bare soil wetting states.

An approach for crops that in their maximum crop development fully cover the soil, like wheat, corn, barley,…, can be stated as:

$$K_c = 1.25\ NDVI + 0.1 \quad (2.10)$$

where

K_c "spectral" crop coefficient [0.15 – 1.20],

NDVI, calculated from surface reflectances on TM and ETM+ bands. [Typical range values: bare soil 0.12-0.16; maximum NDVI value for very dense green vegetation, 0.91]

The bandwidths in the red and NIR bands of OLI sensor onboard of Landsat8 platform are narrower than ETM+ sensor on board of Landsat7. Then, a slightly correction is needed to account the NDVI shift due to the different bandwidths. Then, having in account the higher value of NDVI_L8 for very dense green vegetation which happens at ≈100% green cover, the relationships can be stated as:

So, for the basal crop coefficient, K_{cb},

$$K_{cb} = 1.40\ NDVI_{L8} - 0.15 \quad (2.11)$$

where

K_{cb} "spectral" basal crop coefficient [0.15 – 1.15],

NDVI, calculated from surface reflectances from OLI sensor bands on board of Landsat8 platform. [Typical range values: bare soil 0.12-0.16; maximum NDVI value for very dense green vegetation, 0.935]

An approach for the single crop coefficient, K_c,

$$K_c = 1.2\ NDVI_{L8} + 0.1 \quad (2.12)$$

where

K_c "spectral" crop coefficient [0.15 – 1.2],

NDVI, calculated from surface reflectance on OLI sensor bands on board of Landsat8 platform . [Typical range values: bare soil 0.12-0.16; maximum NDVI value for very dense green vegetation, 0.935]

2.2.2 K_c-NDVI approach set in Greek site by Landsat 8

The calculation of the K_c is can be described with a number of complex equations based on LAI and fPAR inputs. In this paragraph the K_c is calculated from NDVI which is a modified version of the following equation built in Pleiades EU project [18], [19]; [20]) (Figure 2.3).

$$K_c = 1.15 * NDVI + 0.17 \quad (2.13)$$

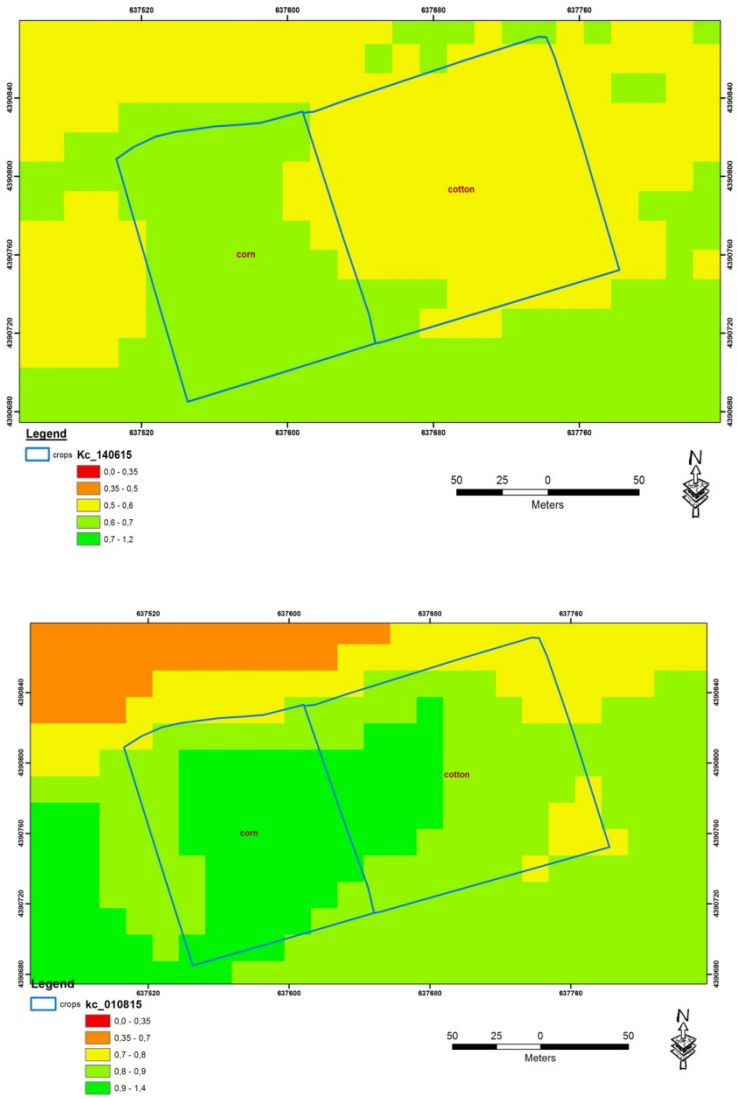

Figure 2.3 - The Kc classified values distribution, for the Landsat-8 images on June 14th and August 1st 2015, respectively

2.2.3 K_C- Red-edge NDVI approach set in Greek site using WV-2 images

In the case of WV-2 it is possible to estimate NDVI from a variety of novel spectral band combinations (e.g., [55]). Ground-truth validation tests are being performed in the Greek pilot area in order to determine the equation (combination of spectral bands) that is most suitable for the subsequent calculation of K_c. The same ground truth validation exercise is also aiming at calibrating the empirical K_c-NDVI relation for the relevant crops and conditions.

This implies using modified versions of the equation (2.14) (same as used with Landsat8-derived NDVI):

$$K_c = 1.15 * NDVI + 0.17 \quad (2.14)$$

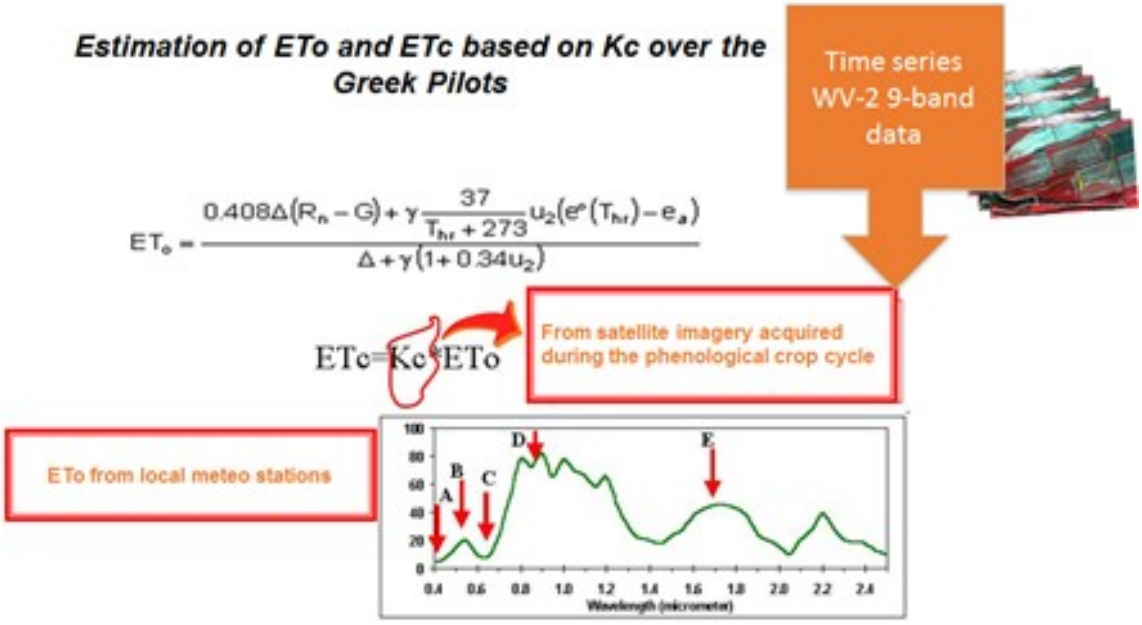

Figure 2.4 - The role of Kc in the estimation of Evapotranspiration

2.3 ET_p direct calculation, based on the application of the Penman- Monteith equation

In direct calculation, ETp can be estimated by the Penman Monteith equation, explicitly written in terms of albedo α, Leaf Area Index (LAI) and meteorological data:

$$ET_p = \frac{86400}{\lambda}\left[\frac{\Delta\left[\left((1-\alpha)R_s - R_{nl}\right) - \left(1-0.4e^{-0.5LAI}\right)\right] + \rho c_p (e_s - e_a)/r_a}{\Delta + \gamma\left(1 + r_{c,min}/r_a\right)}\right]$$

(2.15)

Where:

Meteorological parameters:

λ is the latent heat of vaporization [MJ kg^{-1}], Δ is the slope of saturation vapour pressure curve at air temperature T [kPa $°C^{-1}$], R_s is the incoming solar radiation [MJ m^{-2} day^{-1}], R_{nl} is the net outgoing longwave radiation [MJ m^{-2} day^{-1}], c_p is the specific heat at constant pressure [MJ kg^{-1} $°C^{-1}$], ρ the mean air density at constant pressure [kg m^{-3}], ($e_s - e_a$) is the vapour pressure deficit [kPa], γ is the psychrometric constant [kPa $°C^{-1}$].

Canopy parameters:

- α is the albedo or canopy reflection coefficient;
- $r_{c,min} = \frac{r_s}{LAI_{eff}} \begin{cases} LAI < 0.5\ LAI_{max} \rightarrow LAI_{eff} = LAI \\ LAI > 0.5\ LAI_{max} \rightarrow LAI_{eff} = 0.5\ LAI_{max} \end{cases}$

(2.16)

- $r_s = \begin{cases} 100\ in\ case\ of\ herbaceous\ crops \\ > 400\ in\ case\ of\ tree\ crops \end{cases}$

(2.17)

- $r_a = \frac{ln\left(\frac{z_U - 2/3 h_c}{0.123 h_c}\right) ln\left(\frac{z_T - 2/3 h_c}{0.123 h_c}\right)}{0.168 U}$

(2.18)

- U is wind speed [m s^{-1}].; z_U [m] is the wind measuring height and z_T [m] is the thermo-hygrometric measuring height.

When the soil is not full covered it possible to partition Et_p in soil evaporation and crop transpirations by a well-known model by [21]

$$E_s = ET_p e^{-0.5LAI}$$

(2.19)

$$T_p = ET_p - E_{s,p} = ET_p \left(1 - e^{-0.5LAI}\right)$$

(2.20)

2.3.1 Description of the processing chain and data used

The numbered sequence of elaborations for deriving E.O.-based crop development maps is shown in the box (b) of Figure 2.5

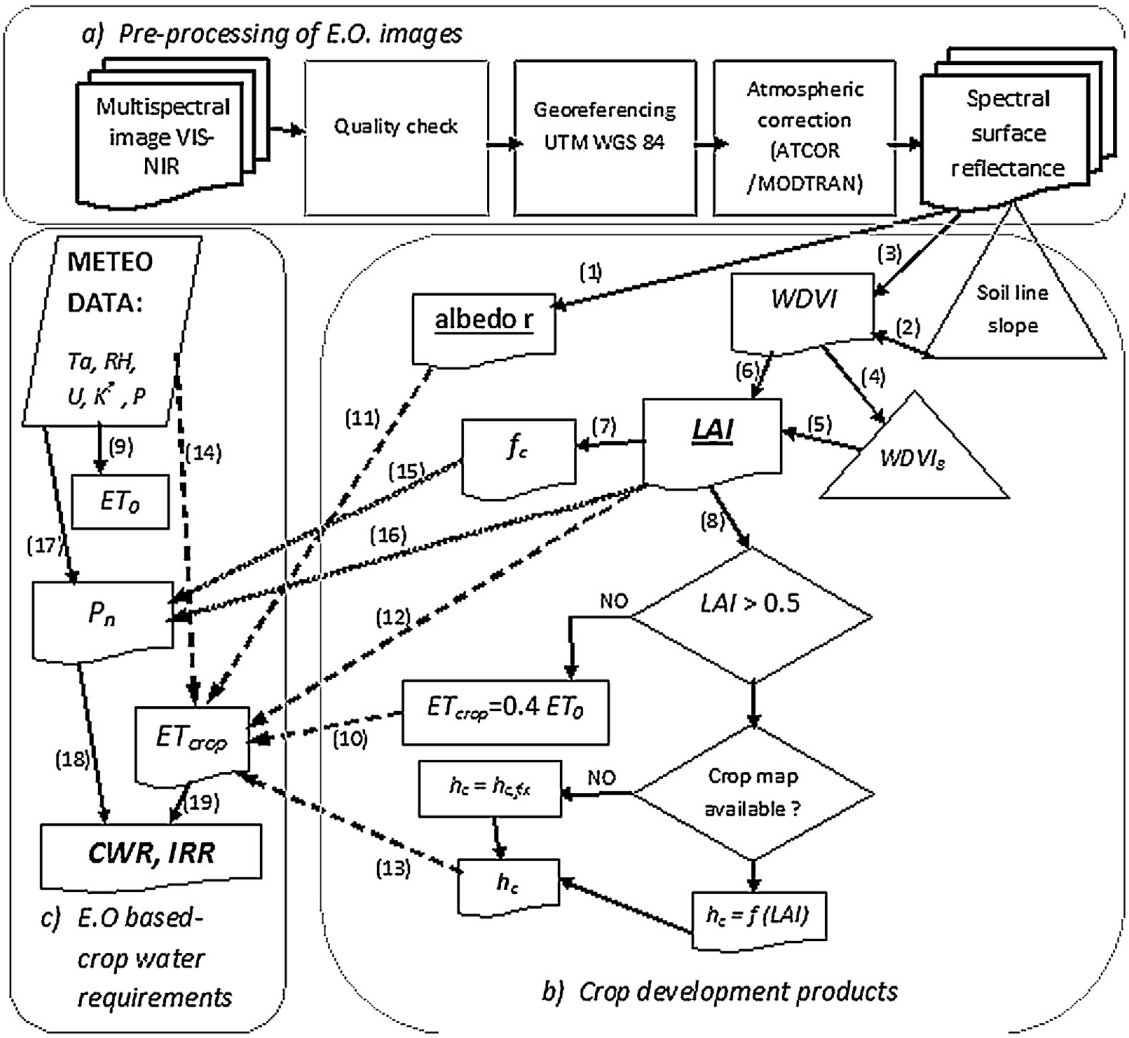

Figure 2.5 - Flow-chart of the processing chain after image delivery. [22]

The albedo needed for deriving the net radiant flux in Eq.(3.15) is an approximation of the hemispherical and spectrally integrated surface albedo; considering the limited spectral resolution of E.O. data normally available, the albedo is calculated as a weighted sum of surface spectral reflectance ρ_λ derived from the atmospheric correction, with broadband coefficients w_λ representing the corresponding fraction of the solar irradiance in each sensor band.

$$r = \sum_{\lambda=1}^{n} \rho_\lambda w_\lambda \tag{2.21}$$

The Leaf Area Index is derived from surface reflectance by applying the model CLAIR [23]

$$LAI = -\frac{1}{\alpha} \ln\left(1 - \frac{WDVI}{WDVI_\infty}\right) \tag{2.22}$$

where α is an empirical shape parameter, mainly depending on canopy architecture, which is determined from field measurements (as shown later, 0.34-0.35 for Italy and Austria and 0.22 for Australia, with prevailing tree crops); WDVI is the Weighted Difference Vegetation Index, and $WDVI_\infty$ is the asymptotic valued for LAI→∞. The WDVI is given by:

$$WDVI = \rho_{NIR} - \rho_{red}\frac{\rho_{s,NIR}}{\rho_{s,red}} \tag{2.23}$$

Hence, the analytical procedure for producing LAI maps from satellite-based images of spectral surface reflectance can be summarised in the following steps:

- identification of the soil-line slope (ratio of average bare soil reflectance in NIR and red bands $\rho_{s,NIR}$, $\rho_{s,red}$ usually between 0.9 and 1.3);
- calculation of the Weighted Difference Vegetation Index WDVI by means of Eq.(2.23);
- identification of $WDVI_\infty$ in correspondence of pixels with maximum vegetation cover (usually between 0.55 and 0.75);
- calculation of LAI by means of Eq.(2.22).

It should be noticed that the selection and utilization of image-based parameters such as the soil line slope and $WDVI_\infty$ may allow for a detection and partial compensation of existing errors in the atmospheric correction procedure, in the case that they are resulting outside the intervals given above.

The fractional vegetation cover f_c is derived from LAI by using a polynomial empirical expression, which coefficients are determined from field measurements and are valid for a wide range of crops:

$$f_c = -0.0038LAI^4 + 0.054LAI^3 - 0.30LAI^2 + 0.82LAI \qquad \forall\, LAI \leq 5 \tag{2.24}$$

Crop height h_c can be derived in a similar way, but a crop specific relationship has to be determined empirically. When this information or the crop maps are not available, h_c is fixed to 0.4 m. The assumption made is that the influence of crop height h_c on the value of ET_p is small for different LAI values; in the plots of Figure 2.6, it has been compared the calculation of ET_p for h_c=0.4 and 1 m and different LAI values. This comparison suggests that the approximation of h_c fixed is acceptable the considered meteorological conditions, with the radiation term of P-M FAO -first addendum in eq.*(2.15)*- larger than the aerodynamic term. This approximation eliminates the need for crop maps which are not timely available, i.e. classification of E.O. data for this purpose can be done only at the end of the irrigation season.

The canopy parameters r, h_c, LAI can be considered as constant for a time period of approx. 7 days from the date of the satellite overpass (see crop growth model for more specifications). Finally, it is possible to calculate ET_p by using the P-M FAO Eq. (2.15), by using the daily meteorological data observed during the previous 7 days or since the previous satellite acquisition; in a similar way, the net precipitation P_n is derived from eq. (2.7) and the crop water requirements CWR from eq. (2.6). The pixel-based *CWR* map is transformed into a vector map by means of digitized plot boundaries. The resulting irrigation advice for the generic plot *i* is then calculated from a simple water balance which on a given day *j* writes as follows:

$$d_{i,j} = d_{i,j-1} + \frac{IRR_{i,j-1}}{\eta_i} - CWR_{i,j-1}$$

(2.25)

with $IRR_{i,j-1}$ representing the irrigation depth in plot *i* on the previous day, $d_{i,j}$ the soil water depletion (starting from a given initial value of day 0) and η_i the on-farm irrigation efficiency (where information on the irrigation methods is available). In the simplest form, i.e. when no additional information on soil properties and local hydrological conditions is known, the maximum irrigation depth is given by:

$$IRR_{i,j} = -d_{i,j} \qquad d_{i,j} < 0$$

(2.26)

$$IRR_{i,j} = 0 \qquad d_{i,j} \geq 0$$

(2.27)

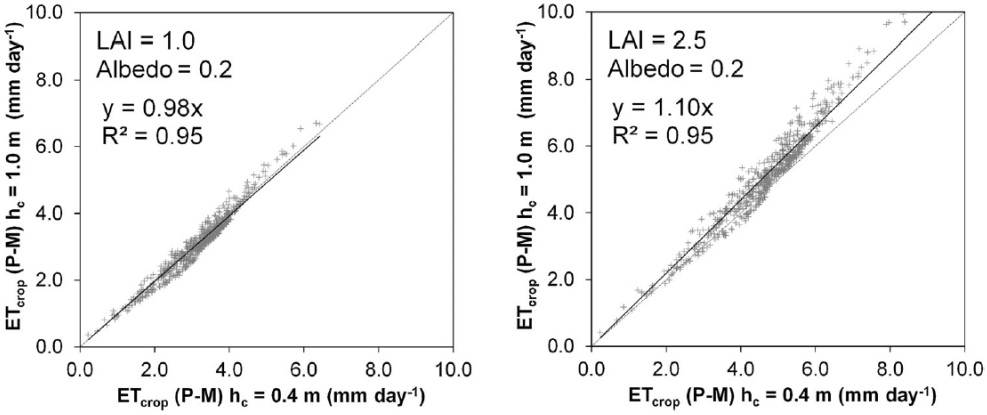

Figure 2.6 - Comparison of evapotranspiration ETp, calculated for five years of summer daily meteo data by using Eq. (2.15), Sele plain, Campania, Italy, for hc= 0.4 and 1 m and twodifferent LAI values. [22]

3 Methodology for EO-based crop and soil water balance

3.1 Background on water balance models

The soil water balance model in irrigation scheduling applications aims at estimating the soil water deficit, and the consequent amount of irrigation to be added. The variation of soil water content $\vartheta(z,t)$ ($cm^3\ cm^{-3}$) during a given time interval Δt over the soil profile between z and $z = 0$ can be expressed by the integral relationship:

$$\int_0^z \left[\theta(z,t+\Delta t)-\theta(z,t)\right] dz = \Delta W = \left(P_n + I_n - E_s - T + v\right)\Delta t \tag{3.1}$$

Eq.(3.1) is the continuity equation in finite differences for a given soil profile, where ΔW is the change in soil water storage, P_n and I_n are respectively the precipitation and irrigation rates actually infiltrating through the soil surface, E_s is the actual evaporation rate from the soil, T is the actual transpiration rate from the crop and v is the water flux density (which can be upward or downward) through the bottom of the soil profile. During the last four decades, the development of sophisticated models for the simulation of water flow in the soil-crop system has been possible thanks to a better knowledge of the physical processes involved and to the possibility of solving automatically complex numerical algorithms. Simulation models validated by means of experimental data in different environments can be used in the practical solution of many problems related to the management of water resources of regional areas. However, the unsaturated soil zone is a complicated dynamical system governed by highly non-linear processes and interactions. Modern sensors are available to quantify flow processes, which can be described by means of physical-mathematical models. Unsaturated-zone numerical models can be used to estimating the timing of irrigations and irrigation depths, drain spacing and drain depth, and to simulate the system behavior and response. Different criteria are used in soil water flow models to establish the start of irrigation and the optimal supply of water. In a simplified way these criteria take into account the response of crops to water stress under soil water deficit conditions. The irrigation criteria contribute to establish an objective, yet theoretical, amount of water needed for irrigation on a given day.

A simulation model can be generally categorized into classes referred to as mechanistic, stochastic, empirical and functional. Each model has its strengths, weaknesses and data requirements and a universally appropriate and versatile model does not exist. The selection of a certain model should depend on the specific task. Intercomparison studies have assessed the performance of some soil water flow models and have provided guidelines to the potential user community on various 'to do' and 'not to do' aspects of specific models (e.g. [24],[25], [26], [27], [28] [29], [30] and [31]). In general, most models perform well, provided detailed field and experimental data to calibrate them. The public expectations concerning environmental and water-resources management within irrigation and drainage projects are extremely high, so that computational tools are needed to assist human intuition in the management of these systems.

Table 3.1 - A selection of various categories of deterministic models for the unsaturated zone that are suitable to describe irrigation and drainage processes (the models and corresponding authors are listed in chronological sequence)

Model category	Example models	Sources
Bucket model	*sowatet, cropwat, salbal, saltmod, wsbm, opdm, cropsim*	Hanks and Cui (1991); Smith (1992a) & Allen et al. (1998); Boumans and Croon (1993); Oosterbaan (1998); Droogers et al. (2001b); Merkley (1996); Prajamwong et al. (1999)
Richards equation	*swatre, drainmod, unsat2, worm, leachm, drainmod-s, isareg, opus, drainet, hyswasor, wave, mozart, swap, hydrus, dssat, cropgro, cropsyst, swms_3d, swat, simodis*	Feddes et al. (1978) & Belmans et al. (1983); Skaggs (1978); Neuman et al. (1974); Van Genuchten (1987); Wagenet and Hutson (1989); Abdel Dayem and Skaggs (1990) & Kandil et al. (1993); Teixeira and Pereira (1992); Smith (1992b); Hundertmark et al. (1993); Yang and Zhang (1993); Dirksen et al. (1993); Vanclooster et al. (1994); Leeuw and Arnold (1996); Van Dam et al. (1997); Sumenick et al. (1998); Ritchie (1998), Hoogenboom et al. (1992) ; Stockle et al. (1994) ; Simunek et al. (1995); Arnold et al. (1999); D'Urso (2001)

3.1.1 Static modelling approach (bucket concept)

Early (but still most commonly used) models of soil water balance used for irrigation scheduling ([32]; [33];) introducing several simplifications in the calculation of Eq.(1). In this type of models, the soil profile is described as a *reservoir* of given capacity W_{max} (bucket concept). The influence of the groundwater flow on the soil water balance, represented by v, is often neglected. Simpler models assume $E_s=E_{s,p}$ and $T=T_p$, being $E_{s,p}$ and T_p respectively the maximum soil evaporation and crop transpiration. In other cases, the actual evapotranspiration rate (E_s+T) is calculated by multiplying E_p with a coefficient that is linearly related to the specific soil water storage W. Irrigation applications are then scheduled when water depletion in the reservoir is larger than a prefixed threshold value. The irrigation volume per unit area is usually taken proportional to the amount of water required to refill the soil to its capacity W_{max} or to a fraction of it. This schematisation is implemented in the FAO-56 model for computing irrigation requirements under "non standard" conditions, i.e. to simulate water stress in the crop. An additional coefficient, k_s, is introduced in the estimation of ET, which value is linked to simulated soil water depletion deriving from the water balance model. The amount of irrigation to be added is a fraction of depletion dependent on crop type, which on turn also defines the root zone depth. The main input for soil is the soil capacity W_{max}, usually determined from soil physical properties, such as texture and particle size distribution, and its depth. Assumptions are needed for the water flux through the bottom boundary of the soil profile, but in most cases it is considered null.

3.1.2 Dynamic modelling approach (Richards equation)

The progress during the last four decades in the knowledge of water flow in the soil-crop-atmosphere system has led to the development of mathematical models for the numerical simulation of water flow

dynamics. If carefully calibrated and validated, these models allow for a much better estimation of water balance terms than reservoir models and they can be used in the practical solution of problems related to the precision management of water resources.

In these models, the soil reservoir is a dynamic *continuum*, where the water flow in the soil-plant-atmosphere system is described. The behaviour of this system, often indicated with the acronym SPAC (Soil-Plant-Atmosphere Continuum), is determined by the soil hydraulic properties, the plant root water uptake, the initial soil moisture distribution and from the surface and bottom boundary conditions. When unsaturated conditions prevail in a large portion of the soil profile, such as in irrigated areas and semi-arid regions, water flow is mainly in the vertical direction. The temporal variation of soil water content $\vartheta(z,t)$ at a given depth can be described by means of the following differential equation ([34]; [25]):

$$\frac{\partial \theta}{\partial t} = \frac{\partial}{\partial z}\left[k(h)\cdot\left(1+\frac{\partial h}{\partial z}\right)\right] - S \qquad (3.2)$$

where $k(h)$ (cm d-1) is the unsaturated hydraulic conductivity, h is the soil water pressure head, z is the vertical coordinate (positive upward) and S is the *water uptake by roots* per unit volume of soil per time ($cm^3cm^{-3}d^{-1}$). This equation results from the combination of the mass conservation equation and the equation of Darcy extended for water unsaturated soils [34]. According to the model proposed by [35], root water uptake S can be described as a function of h:

$$S = S(h) = \alpha(h) S_{\max} = \alpha(h)\frac{T_p}{z_r} \qquad (3.3)$$

with z_r (cm) being the thickness of the root zone and $\alpha(h)$ a semi-empirical function of pressure head h. As shown in Figure 3.1, the shape of the function $\alpha(h)$ depends on four critical values of h, which are related to the type of crop and to the potential transpiration rates.

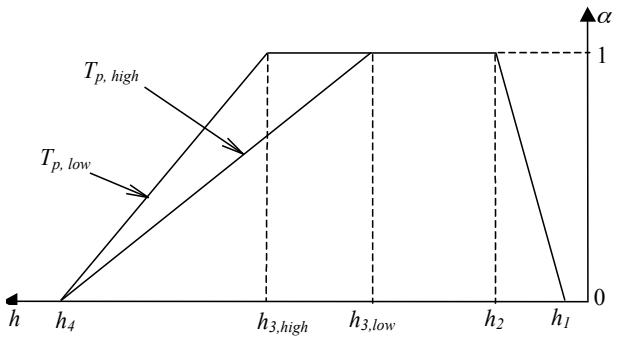

Figure 3.1 - Root water uptake function α(h); the critical values of pressure head h are crop-dependent; h3 has two different values respectively for high and low potential transpiration rate .

Eqs.(2-3) are the basic relationships of the agrohydrological simulation tool named SWAP [36]. They are solved to determine the vertical distributions of pressure head $h(z,t)$ and soil water content $\vartheta(z,t)$ and all the terms of water balance for each time step. This requires the definition of the initial condition, that is the distribution $h(z,t = 0)$ or $\vartheta(z,t = 0)$, and the conditions on the boundaries, at $z = 0$ and $z = -z^*$, $\forall\ t > 0$.

The analysis of the distributions *h(z,t)* and *ϑ(z,t)* is a valuable guidance for irrigation scheduling and several applications at farm scale are reported in literature ([37]; [38]; [39]). Irrigation schedules and volumes can be fixed according to the values of *ϑ* and *h* in the root zone [36]. In a given time, the soil water deficit *δ* (cm) in the soil profile between *z* and *z* +*Δz* is given by the expression:

$$\delta = \int_{z}^{z+\Delta z} \left[\theta_s(z) - \theta(z)\right] \; dz$$

(3.4)

where ϑ_s the water content near saturation. The irrigation water volume to be applied can be either a prefixed amount or it is calculated as a fraction i_r of the soil water deficit *δ*. In this latter case the irrigation volume $\boldsymbol{I}_0$ (m^3), net of water losses due to on-farm distribution equipment, is:

$$\boldsymbol{I}_0 = 100\, i_r \delta A$$

(3.5)

where A is the irrigated area (ha). The value of i_r depends on the irrigation criteria adopted by individual farmers and it can be determined from field measurements of irrigation volumes applied in coincidence of simulated or measured soil water deficit. An example of calculated profiles of *h(z,t)* and *ϑ(z,t)* is given in Figure 3.2. The simulation refers to a three-layered soil, with a ground water table at 2 m depth. In this example, the assumed threshold is h_{crit}= -500 cm. At time *t* the average pressure head in a portion of soil profile, i.e. the root zone between z_1 and z_2, has a value of -636 cm, which is lower than h_{crit} (**¡Error! No se encuentra el origen de la referencia.**ft). When this condition occurs, irrigation should be applied. At the same instant *t*, the soil water deficit respect is equal to 6.5 cm (Figure 3.2 right). Assuming i_r=0.4, the irrigation volume per unit area in this case is 2.6 cm.

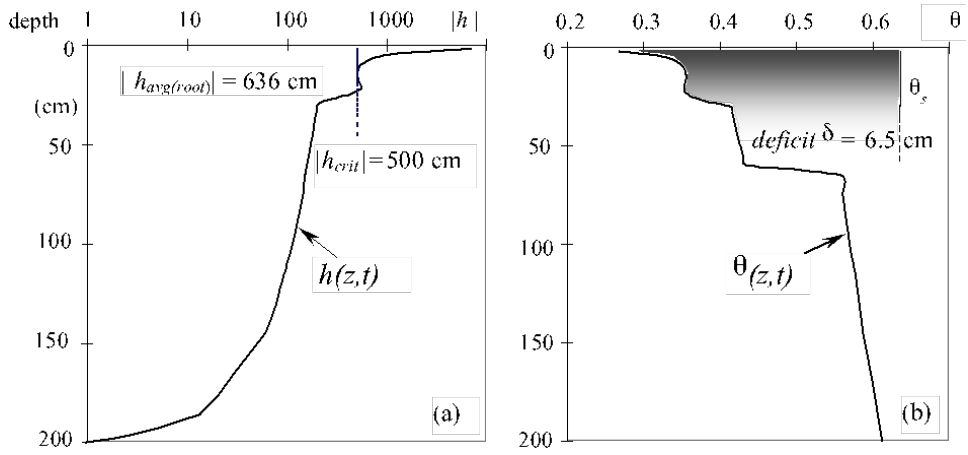

Figure 3.2 - Example of SWAP output concerning the vertical distribution of pressure head h (left) and soil water content ϑ (right) in a three-layered profile with the ground water table at 2 m depth at time t. Critical values of pressure head and soil water deficit in the root zone are used to determine irrigation schedules and amounts

The boundary conditions for the solution of Eqs.(2-3) are depending on the potential soil evaporation rate and the amount of intercepted precipitation as determined by the vegetation cover at the soil surface and by the climatic variables. Among the variables describing the vegetation cover, K_c and *LAI* have the largest

impact on the upper boundary condition. In particular, the *LAI* is used to estimate the soil evaporation, the canopy transpiration, and the amount of precipitation and irrigation water intercepted by the canopy. The semi-empirical model of interception described by [6] can be applied for this purpose; this model is expressed by the relationship:

$$P_n = P - aLAI\left(1 - \frac{1}{1 + \frac{s_c \cdot P}{aLAI}}\right) \tag{3.6}$$

where P is the precipitation above the canopy (cm d^{-1}), a (cm d^{-1}) is an empirical parameter representing the crop saturation per unit foliage area (≈0.28 for most crops) and s_c (-) is the fractional vegetation cover, which can be related to *LAI* by means of empirical relationships. A similar relationship can be used to estimate I_n where P is substituted by (***I/A***).

The boundary condition at the *bottom* of the considered one-dimensional soil column can be defined in three ways by specifying: i) a value of the pressure head at the bottom or a groundwater table depth, ii) a fixed flux density through the bottom, or iii) a flux density through the bottom as a function of groundwater table depth. The first type of condition is often used when groundwater depths recordings are available. This type of condition, however, can not be used in scenario simulations, unless the water table depth is artificially fixed. The second option may be taken when it is possible to identify an impermeable layer, which determines a "zero" flux, or when the water table is deep enough to leave the soil profile unsaturated, so that the percolation flux density equals the value of hydraulic conductivity for the prevailing pressure head at the bottom (unit gradient). This option is equivalent to the one most commonly used in bucket models. The third one can be identified by means of field observations of groundwater table.

The amount of input data required for these type of models is generally more complex than the simpler bucket models; however, the utilisation of pedo-transfer functions (REF TO BE ADDED) and the availability of ample and reliable literature data for crop parameters (including the stress potentials in Figure 3.1) are available. Suitable calibration is needed to assess the accuracy of the simulation results. Respect to bucket models, dynamic models allow for taking into account more accurately the conditions for water stress and they avoid strong assumptions about the actual water uptaking of crops and the fluxes through the bottom boundary of the soil profile.

4 Application of numerical weather prediction (NWP) models for forecasting crop evapotranspiration

4.1 Weather forecasts for agriculture

Weather plays an important role in agricultural production. It has a profound influence on crop growth, development and yields; on the incidence of pests and diseases; on water needs; and on fertilizer requirements. This is due to differences in nutrient mobilization as a result of water stresses, as well as the timeliness and effectiveness of preventive measures and cultural operations with crops. Weather factors contribute to optimal crop growth, development and yield. They also play a role in the incidence and spread of pests and diseases. Susceptibility to weather induced stresses and affliction by pests and diseases varies among crops, among different varieties within the same crop, and among different growth stages within the same crop variety [40]. Despite careful agronomic planning on a microscale to suit experience in local-climate crops, various types of weather events exist on a year-to-year basis. Deviations from normal weather occur with higher frequencies in almost all years, areas and seasons. The most common ones are a delay in the start of the crop season due to rainfall vagaries in the case of rainfed crops (as observed in the semi-arid tropics) and temperature (as observed in the tropics, temperate zones and subtropics), or persistence of end-of-the season rains in the case of irrigated crops. Other important phenomena are deviations from the normal features in the temporal march of various weather elements. The effects of weather events on crops build up slowly but are often widespread. Thus, there is no aspect of crop culture that is immune to the impact of weather. For these reasons, if a forecast of the expected weather can be obtained in time, it is possible to adapt to or mitigate the effects of adverse weather conditions. Moreover a high forecast resolution operationally independent can add a substantial value to the precision of the agricultural advice.

4.2 Numerical weather prediction (NWP) models

The term “numerical weather prediction” (NWP) refers to those weather forecasts based on the output of numerical models which simulate the processes governing the dynamical evolution of the state variables characterizing the physical conditions of the atmosphere and of the surface of the oceans. [41]. The model formulation is based on a set of primitive equations: some of these equations are diagnostic, describing the static relationship between pressure, density, temperature and height and other equations are prognostic, describing the time evolution of the horizontal wind components, surface pressure, 3D temperature and the water vapour contents of an air parcel. The main prognostic equations are the Navier–Stokes equations on a rotating sphere with thermodynamic terms for various energy sources (radiation, latent heat). Other specific equations are used to predict the hydrometeors and the changes in the physical characteristics (rain, snow, liquid water, cloud ice content etc.)

Classical predictability theory suggests that the upper limit of skillful daily forecasts may be realized up to two weeks ahead [42]. However, model integrations with perturbed initial conditions diverge rapidly and produce different forecasts.

Such are the drawbacks of numerical weather prediction and weather forecasting in general – the farther you attempt to forecast into the future, the more difficult it is to predict details about an atmospheric "stick" (a metaphor for weather systems such as a mid-latitude low) that moves within the fast currents of the jet stream. Medium-range forecasts in fast-flow patterns during the cold season are particularly prone to error. These forecasting limitations are especially true in medium-range forecasting (the medium range generally represents three to seven days in the future). It is suggested that a WRF model is deployed aiming in covering a 6x6 resolution in the areas of interest and in making data available for the SPIDER system, in various formats working in an operational mode provided that data needed for the initiation of the model are available. The following table depicts the advantages of the WRF model in comparison with the current available solutions

Table 4.1 - advantages of the WRF model in comparison with the current available solutions ***Forecast Characteristics***	**Forecast Providers**		
	ECMWF	**NCEP**	**FATIMA METEO TOOL**
Spatial Resolution	$0.125^{o}\times0.125^{o}$	$0.25^{o}\times0.25^{o}$	**$0.06^{o}\times0.06^{o}$**
Geographical Coverage	Global	Global	Europe
Temporal Resolution	3h	1h (first 24h)-3h	1h
Forecast Cycles	00UTC, 12UTC	00UTC, 06UTC, 12UTC, 18UTC	12UTC
Forecast Horizon	10days	10days	**7days**
Data Format	GRIB2	GRIB2	**GRIB2, NETCDF, Raster, ASCII etc.**
FAO56 Reference Evapotranspiration	**No**	**No**	**Yes**
Precipitation	Yes	Yes	Yes
Temperature 2m	Yes	Yes	Yes
Dew point Temperature	Yes	Yes	Yes
2m Wind Speed	No (10m Wind Speed)	No (10m Wind Speed)	**Yes**
Total Solar Radiation	Yes	Yes	Yes
Photosynthetic Active Radiation	Yes	Yes	Yes
Correction Method	No	No	**MOS (Model Output Statistics).**

4.3 Domain Coverage: General Circulation Models (GCM) and Limited Area Models (LAM)

Based on the domain coverage, NWP models are divided into *General Circulation Models (GCM)* and *limited area models (LAM)*. Global models solve the primitive equations for the whole globe while limited area models cover only a limited domain.

The atmospheric general circulation model describes the dynamical evolution on the resolved scale and is augmented by the physical parameterization, describing the mean effect of sub-grid processes and the land-surface model; coupled to this is an ocean wave model [43]. Additional equations describe changes in the hydrometeors (rain, snow, liquid water, cloud ice content etc). There are options for passive tracers such as ozone. The processes of radiation, gravity wave drag, vertical turbulence, convection, clouds and surface interaction are, due to their relatively small scales (unresolved by the model's resolution), described in a statistical way as parameterization processes (arranged in entirely vertical columns).

The model equations are discretized in space and time and solved numerically by a semi-Lagrangian advection scheme. It ensures stability and accuracy, while using as large time-steps as possible to progress the computation of the forecast within an acceptable time. For the horizontal representation a dual representation of spectral components and grid points is used. All fields are described in grid point space. Due to the convergence of the meridians, computational time can be saved by applying a "reduced Gaussian grid". This keeps the east-west separation between points almost constant by gradually decreasing the number of grid points towards the poles, at every latitude in the extra-tropics. For the convenience of computing horizontal derivatives and to facilitate the time-stepping scheme, a spectral representation, based on a series expansion of spherical harmonics, is used for a subset of the prognostic variables. The vertical resolution is finest in geometric height in the planetary boundary layer and coarsest near the model top. The "σ-levels" follow the earth's surface in the lower-most troposphere, where the Earth's orography displays large variations. In the upper stratosphere and lower mesosphere they are surfaces of constant pressure with a smooth transition in between.

Because of the high costin computational resources, few meteorological centers run global models. German meteorological center runs a global model (GME) with 40 km horizontal resolution and 40 verticallevels, National Center for Environmental Prediction NCEP/NOAA also runs a global model with 13 km resolution, European Centre for Medium-Range Weather Forecasts (ECMWF) is running an operational global model with 12.5 km resolution. Because of their relative low resolution, global models cannot resolved explicitly small scale phenomena such as orographical induced convection, temperature inversion etc. The Table 4.2 - shows most of providers of the Global Models.

Table 4.2 - Global Model Providers

Data provider	
BoM (ammc)	Bureau of Meteorology, Melbourne, Australia
CMA (babj)	China Meteorological Administration, Beijing, China
CMC (cwao)	Meteorological Service of Canada, Montreal, Canada
CPTEC (sbsj)	Centro de Previsao Tempo e Estudos Climaticos, Cachoeira Paulista, Brazil
ECMWF (ecmf)	European Centre for Medium-Range Weather Forecasts, Reading, Europe
JMA (rjtd)	Japan Meteorological Agency, Tokyo, Japan
KMA (rksl)	Korea Meteorological Administration, Seoul, Korea
MeteoFrance (lfpw)	MeteoFrance, Toulouse, France
MetOffice (egrr)	MetOffice, Exeter, United Kingdom
NCEP (kwbc)	National Centres for Environmental Prediction, Washington, DC, USA National Oceanic and Atmospheric Administration, Washington, DC, USA

In order to cover the country domain, many national meteorological departments or agency started running limited area models (LAMs) which can run at high resolution (< 10 km). Compared to global models, LAMs are typically used to predict mesoscale weather phenomena. Due to the limited area coverage, LAM models need initial and boundary conditions from global models. Different LAM models differ for numerical formulation, assumptions, equation simplifications, domain and resolution. Table 4.3 - Most Limited Area Models.

Table 4.3 - Most Limited Area Models

WRF-NMM	The WRF Nonhydrostatic Mesoscale Model was the primary short-term weather forecast model for the U.S., replacing the Eta model.
WRF-ARW	WRF-ARW Advanced Research WRF developed primarily at the U.S. National Center for Atmospheric Research (NCAR) is a state of the art numerical weather prediction model, applicable for both research and operational forecasting purposes.
WRF-METEO-TOOL	A numerical weather prediction service based on WRF-ARW model. Provides hourly reference evapotranspiration and precipitation data, covering Europe and the Mediterranean Countries with a spatial resolution of 6x6 km. The forecast horizon is 7 days ahead.
NAM	The term North American Mesoscale model refers to whatever regional model NCEP operates over the North American domain. NCEP began using this designation system in January 2005. Between January 2005 and May 2006 the Eta model used this designation. Beginning in May 2006, NCEP began to use the WRF-NMM as the operational NAM since 2011 and from 2012 it was replaced by the NEMS-NMMB model.
RAMS	Regional Atmospheric Modeling System developed at Colorado State University for numerical simulations of atmospheric meteorology and other environmental phenomena on scales from meters to hundreds of kilometers - now supported in the public domain
MM5	The Fifth Generation Penn State/NCAR Mesoscale Model
ARPS	the Advanced Region Prediction System developed at the University of Oklahoma is a comprehensive multi-scale nonhydrostatic simulation and prediction system that can be used for regional-scale weather prediction up to the tornado-scale simulation and prediction. Advanced radar data assimilation for thunderstorm prediction is a key part of the system..
HIRLAM	HIRLAM High Resolution Limited Area Model
GEM-LAM	GEM-LAM Global Environmental Multiscale Limited Area Model, the high resolution 2.5 km (1.6 mi) GEM by the Meteorological Service of Canada (MSC)
ALADIN	ALADIN The high-resolution limited-area hydrostatic and non-hydrostatic model developed and operated by several European and North African countries under the leadership of Météo-France[40]
COSMO	COSMO The COSMO Model, formerly known as LM, aLMo or LAMI, is a limited-area non-hydrostatic model developed within the framework of the Consortium for Small-Scale Modelling (Germany, Switzerland, Italy, Greece, Poland, Romania, and Russia)

4.3.1 Ensemble forecasting systems

Computer forecasts can go awry for several reasons. For example, they fail if the initialization does not accurately represent the current state of the atmosphere. Meteorologists compensate by implementing a technique that gauges how sensitive computer models are to the way they're initialized. Specifically, forecasters tweak (make minor changes to) the initialization of a model, and then run the model using this slightly different initial state. Then they tweak the initialization again, in a slightly different way, and run the model using this new initial state. This process of "tweaking" the initial conditions is repeated a number of times. If all or most of the tweaked model runs come up with basically the same numerical prediction, for a specific forecast day, meteorologists have a relatively high degree of confidence in that day's forecast. If, however, the tweaked model runs predict several noticeably different scenarios for the day in question, then forecasters have a fairly low degree of confidence in the numerical prediction. The collection of different runs from the series of initialization "tweaks" is called an **ensemble prediction**, and each individual run is an **ensemble member**. Ensemble approaches were introduced in meteorology. The amount of agreement between the members can be considered as a measure of forecast certainty or uncertainty. Ensemble forecasting can quantify the spread of forecast error and assessing the uncertainty propagation in the prediction. Table 4.4 shows most of ensemble model, the number of members (ensemble size), the length of forecast in hours and the time in which models start running every day.

Table 4.4 - Limited Area Ensemble Models

Model	ensemble size	control forecast	forecast length [h]	model runs (1) [UTC]
ALADIN-LAEF	16	yes	72	00,12
COSMO-DE-EPS	20	no	27	00,06,12,18
COSMO-LEPS	16	no	132	00,12
DMI-HIRLAM	25	yes	64	00,06,12,18
GLAMEPS	54	no	60	06,18
HUNEPS	11	yes	60	18
MOGREPS	12	no	36	03,09,15,21
PEARP	35	yes	54	06,18

There are many studies, which suggest the use of Numerical Weather Prediction, NWP, models for ET_0 forecasts ([44]; [45]; [46]; [47]). None of these studies contemplates the use of ensembles of NWP, known as Ensemble Prediction Systems (EPS), which, on the other hand, are widely adopted in different areas of hydrology such as flood forecasting (for a review, see: [48]). EPS are well suited for dealing with initial

condition and model uncertainties in a chaotic environment, such as the atmosphere. From small perturbations applied to the initial conditions and, eventually, to the model parameters, EPS give an ensemble of possible future conditions instead of a deterministic output [49]).

4.4 Operational weather prediction models in Europe: The COSMO-Model

The COSMO-Model is a non-hydrostatic limited-area atmospheric prediction model. It has been designed for both operational numerical weather prediction (NWP) and various scientific applications on the meso-β and meso-γ scales [50]. The COSMO-Model is based on the primitive thermo-hydro-dynamical equations describing compressible flow in a moist atmosphere. The model equations are formulated in rotated geographical coordinates and a generalized terrain following height coordinate. A variety of physical processes are taken into account by parameterization schemes.

Table 4.5 - Details of the coarse applications of all COSMO partners

	Domain Size (grid points)	Hor. Grid Spacing (degree / km)	Number of Layers	Time Step (sec)	Fore-cast Range (h)	Initial Time of Model Runs (UTC)	Lateral Boundary Conditions	LBC Update Freq. (h)	Initial State
ARPA–SIM	297 x 313	0.0625 / 7	40	40	72	00, 12	IFS	1	Nudging Scheme
DWD	665 x 657	0.0625 / 7	40	40	72	00, 06, 12, 18	GME	1	Nudging Scheme
HNMS	649 x 393	0.0625 / 7	60	60	72	00, 12	IFS	3	IFS
IMGW	193 x 161	0.125 / 14	35	80	72	00, 12	GME	1	GME
MeteoSwiss	393 x 338	0.06 / 6.6	60	60	72	00, 06, 12	IFS	1	Nudging Scheme
NMA	201 x 177	0.0625 / 7	40	40	78	00, 12	GME	3	GME
Roshydromet	700 x 620	0.0625 / 7	40	40	78	00, 06, 12, 18	GME	3	GME
USAM	779 x 401	0.0625 / 7	40	40	78	00, 12	IFS	3	CNMCA 3DVAR-FGAT
LEPS	511 x 415	0.0625 / 7	40	60	132	12	IFS-EPS members	3	IFS-EPS members

The basic version of the COSMO-Model (formerly known as Lokal Modell (LM)) has been developed at the Deutscher Wetterdienst (DWD). The COSMO-Model and the triangular mesh global gridpoint model GME form – together with the corresponding data assimilation schemes – the NWP-system at DWD, which is run

operationally since end of 1999. The subsequent developments related to the model have been organized within COSMO, the Consortium for Small-Scale Modelling. COSMO aims at the improvement, maintenance and operational application of a non-hydrostatic limited-area modelling system, which is now consequently called the COSMO-Model.

The COSMO-Model is operated since several years now in the centers of the Consortium for Small-Scale Modelling with moderate resolutions of 7 and 14 km. The boundary conditions for the operational runs with such moderate resolutions are derived from forecasts of the global model GME of DWD. Only a subset of GME data covering the respective COSMO-domain are provided from DWD via the Internet. This ensures an efficient and timely transmission. Alternatively, the global IFS data from ECMWF can be used for boundary conditions. Figure 4.1 show the details and operational domains of the coarse applications of all COSMO partners.

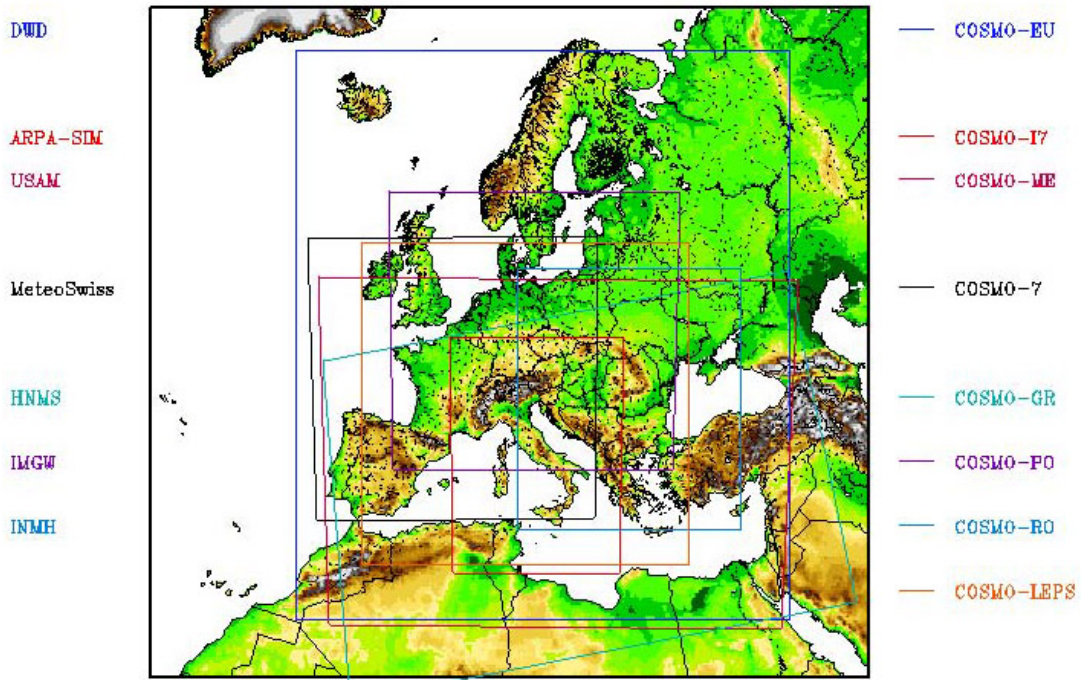

Figure 4.1 - Operational domains of the coarse applications of all COSMO partners

4.5 COSMO-LEPS (Limited Area Ensemble Prediction System)

ARPA-SIM installed the COSMO-LEPS (Limited Area Ensemble Prediction System) based on the COSMO-Model and ECMWF ensemble forecasts at the ECMWF computing centre. 16 operational model runs are performed (7 km grid spacing, 40 levels forecast range of 132 hours) starting at 12 UTC on initial and boundary conditions from 16 representative members of an ECMWF-EPS superensemble. The limited-area ensemble prediction system COSMO-LEPS has been running every day at ECMWF since November 2002. A number of runs of the non-hydrostatic limited-area model Lokal Modell (LM) are available every day, nested on members of the ECMWF global ensemble. The limited-area ensemble forecasts range up to 120 h and LM-based probabilistic products are disseminated to several national and regional weather services.

The system has been designed to have a probabilistic support at the mesoscale, focusing the attention on extreme precipitation events.

COSMO-LEPS application starts at about 20.50 UTC, once the ECMWF EPS starting at 12UTC has passed fc+144h forecast range. Products are disseminated to Met Ops rooms of COSMO weather offices starting from 23.00UTC.

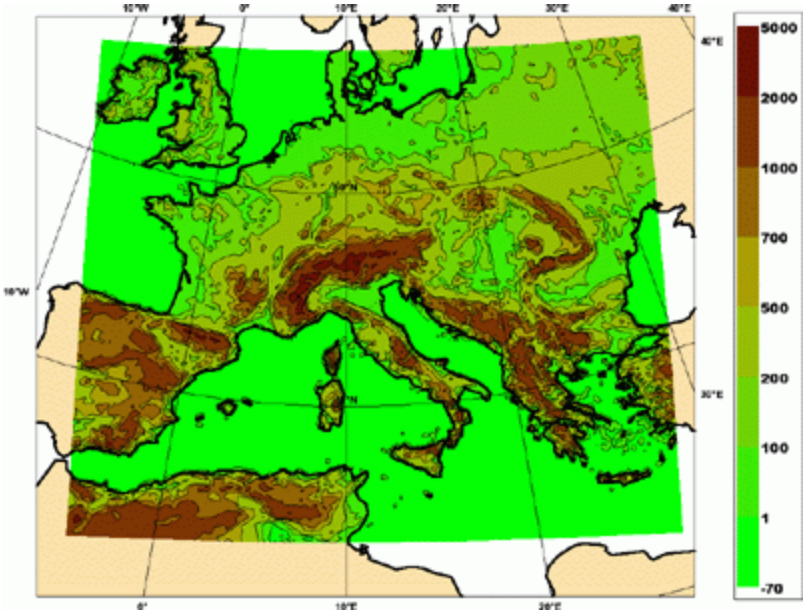

Figure 4.2 - Operational domains of the coarse applications of COSMO-LEPS

4.6 HIRLAM (HIgh Resolution Limited Area Model)

The international research programme HIRLAM (HIgh Resolution Limited Area Model) is a research cooperation of European meteorological institutes. HIRLAM programme aims to develop and maintain a numerical short-range weather forecasting system for operational use by the participating meteorological institutes. The HIRLAM model is a hydrostatic grid-point model, of which the dynamical core is based on a semi-implicit semi-Lagrangian discretisation of the multi-level primitive equations, using a hybrid coordinate in the vertical. Optionally, an Eulerian dynamics scheme can be used as well.

The prognostic variables horizontal wind components u,v, temperature T, specific humidity q and linearised geopotential height G are defined at full model levels. Pressure p, geopotential height Φ and vertical wind velocity are calculated at "half" levels. For the horizontal discretization, an Arakawa C-grid is used. The equations are written for a general map projection, but in practice normally a rotated lat-lon grid projection is utilized. A fourth-order implicit horizontal diffusion is applied. More details on the dynamical and numerical aspects of HIRLAM can be found in [51].

4.7 Fatima-WRF-Meteo-Tool

FATIMA-WRF-ARW is a next generation, state of the art, open source mesoscale numerical model and data assimilation system, designed to serve both operational and atmospheric research needs. Draxis Environmental Technologies S.A. utilizing WRF-ARW in operational mode in order to provide numerical weather prediction services (WRF-METEO-TOOL). WRF-METEO-TOOL provides hourly forecast data of every possible atmospheric variable from the surface up to 20 Km, covering Europe and the Mediterranean Countries at a resolution of 6x6km, for 7 days ahead. In topographical challenging areas WRF-METEO-TOOL is able to improve forecast skill using model output statistics and Kalman filtering techniques in combination with past station data, if they are available. The operational version of the FATIMAmeteo tool will be based on satellite data gathered on a daily basis and analyzed locally in advanced infrastructure dedicated for the specific analysis. The requested ET_0 parameter will be produced in a compatible to SPIDER web-tool temporal and spatial resolution to better match the needs of the holistic FATIMA approach.

4.8 Forecasting reference evapotranspiration with NWP model

The real-time calculation of daily reference evapotranspiration (ET_0), which is the basis for estimating crop evapotranspiration (ET_p), is essential for real-time irrigationscheduling. The FAO Penman–Monteith (FAO-PM) method is recommended as the standard ET_0 method, which the evapotranspiration of a hypothetical reference vegetated field is unambiguously determined [1]. ET_p is computed by multiplying ET_0 with the crop coefficient value K_c, using parameters describing the canopy development, i.e. LAI, surface albedo and crop height. These canopy parameters entering in the direct calculation of ET_p and they can be determined on a pixel-by-pixel basis,using satellite observations in the visible and near-infrared spectral domains.

For daily ET_0 calculation, the FAO-PM method requires daily data on maximum and minimum 2m air temperature (Tmax and Tmin), 2m relative humidity (RH), short wave solar radiation (Rs) and 2m wind speed (u). Unfortunately weather stations are scarce, unevenly distributed and do not always have the instrumentation to measure relevant variables for its calculation. Besides, the forward step is to produce water requirements predictions for the next week. (which needs ET_0 and ET_p forecast). To this end, distributed short term forecasting of relevant meteorological data (from high-resolution limited area weather prediction models) will be used as input in the above mentioned model. Having the knowledge of crop water requirements and by mean of water balance , irrigation volume can be either to satisfy full crop requirements, either to manage under deficit irrigation.

Over the last years there have been improvements in objective weather forecasting based on numerical weather prediction, opening the possibility of applying their outputs for agricultural water management. In fact, these models not only provide forecast for commonly used variables such as temperature and precipitation. They also give information regarding other relevant variables such as pressure, wind speed and direction, specific humidity and solar radiation. All of these variables are required to calculate reference evapotranspiration, representing a potentially valuable source of information for water resources management.

4.8.1 Example of Forecasting reference evapotranspiration (ET0)

Numerical weather model outputs can be efficiently applied for retrieving reliable forecasts of the reference evapotranspiration for optimizing the irrigation scheduling at farm level. In this Section, we compare daily forecasts of reference evapotranspiration (ET0) based on Numerical Weather Prediction Model outputs with daily ET_0 estimates from measured meteorological variables, at sixteen monitoring stations (ground-based automatic weather stations, AWSs) distributed across the Campania Region (Figure 4.3) Southern Italy characterized by dry-summer subtropical climates, which are often referred to as "Mediterranean". The Ensemble Numerical Weather Prediction outputs are those provided by COSMO-LEPS, an Ensemble Limited Area Model operated by ARPA-Emilia Romagna (Italy), with:

- 16 members;
- 7.5 km spatial resolution;
- forecast lead-time up to 5 days.

ET_0 forecasts are computed with three different models: i) FAO Penman–Monteith, ii) Hargreaves-Samani (temperature-based) and iii) Priestley-Taylor (solar radiation-based). These three ET_0 forecasts are respectively compared with the corresponding FAO Penman–Monteith ET_0 estimates obtained with the observed weather variables. The comparison period is from April to September of years 2013 and 2014.

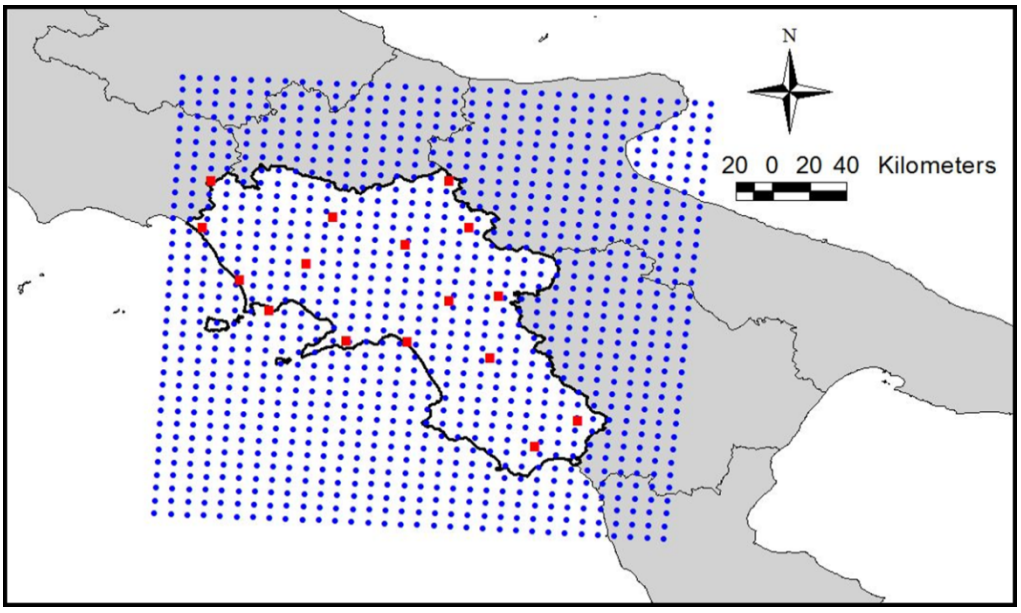

Figure 4.3 - Study area, meteorological stations (red squares) and COSMO-LEPS grid points (blue circles)

4.8.1.1 Comparison

The comparison period is from April to September of years 2013 and 2014. The period from April to September corresponds to the maximum time span of the irrigation season in the study area. In these two periods, the difference between the daily ET_0 calculated using weather forecasts and the daily ET_0

calculated using observed weather data appears to be stochastically independent from the time of the year. Figure 4.4 and Figure 4.5 compare the predicted daily ET_0 (i.e. computed with the three empirical methods) and the observed daily ET_0 at one of the AWS sites (Rocca D'Evandro) for lead times of 1 day and 5 days, respectively. The predicted values (blue continuous line) correspond to the median of the ensemble forecasts. The dotted lines represent the 10^{th} and 90^{th} percentiles of the ensemble. The figures reveal a higher spread of the 10^{th} and 90^{th} percentiles of the ensemble as the lead time increases, as a result of increasing uncertainty of the weather forecasts.

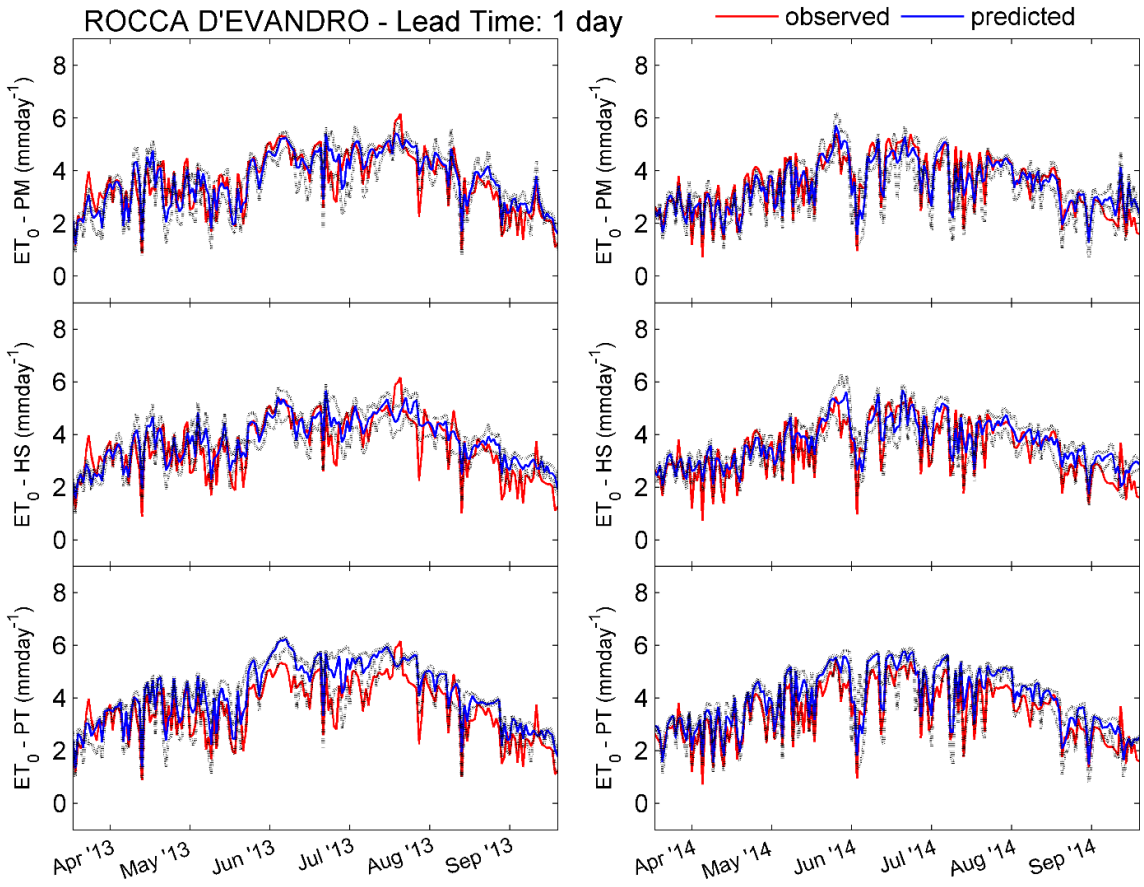

Figure 4.4 - Comparison between the predicted daily ET0 computed by Penman-Monteith (ET0 - PM) Hargreaves-Samani (ET0 - HS) and Priestley-Taylor (ET0 - PT) with observed daily ET0 computed by Penman-Monteith at AWS no. 11 (i.e. Rocca D'Evandro) for 1 day lead time. The predicted values are the median of the ensemble forecasts and the dotted lines refer to the 10th and 90th percentiles.

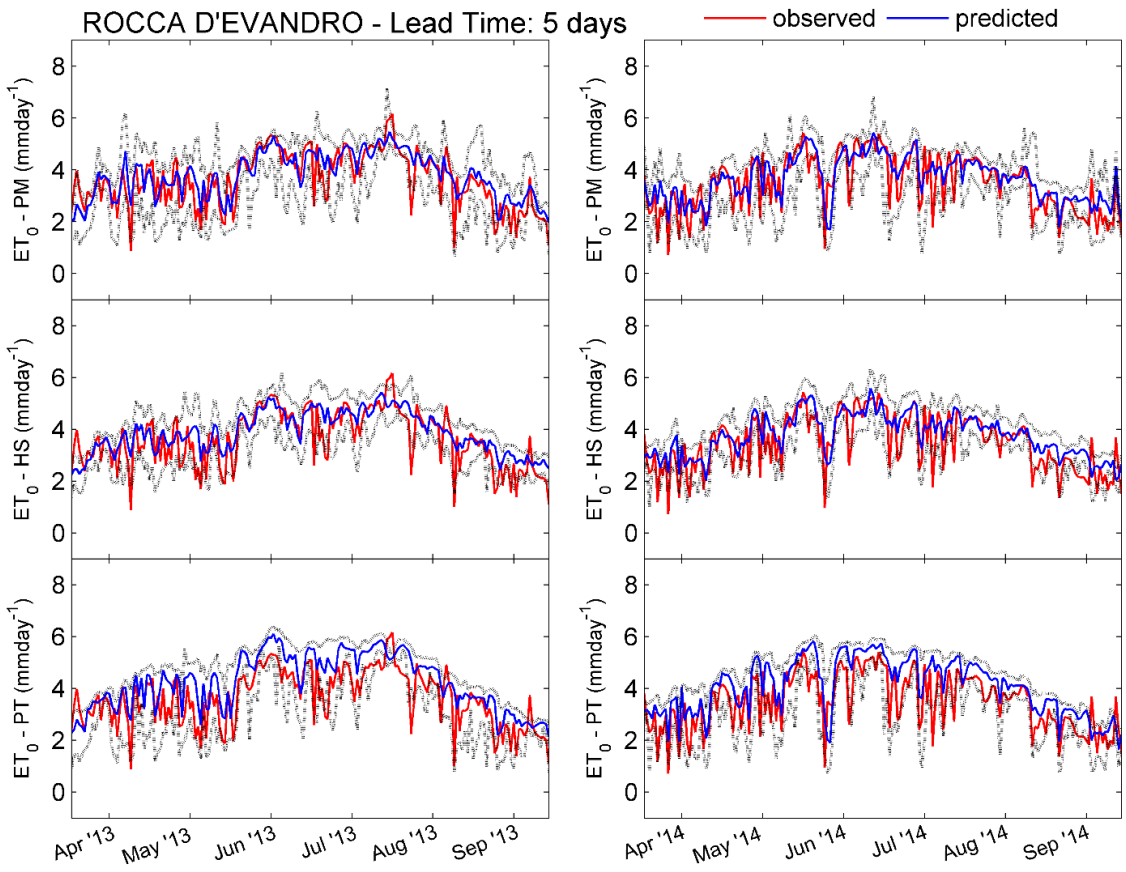

Figure 4.5 - Comparison between the predicted daily ET0 computed by Penman-Monteith (ET0 - PM) Hargreaves-Samani (ET0 - HS) and Priestley-Taylor (ET0 - PT) with observed daily ET0 computed by Penman-Monteith at AWS no. 11 (i.e. Rocca D'Evandro) for 5 days lead time. The predicted values are the median of the ensemble forecasts and the dotted lines refer to the 10th and 90th percentiles.

4.9 Forecasting potential evapotranspiration ET_p using numerical weather prediction (NWP) and assimilating LAI from remote sensing data in crop model with Ensemble Kalman Filter.

The goal of the following procedure is the forecast of the potential evapotranspiration for 5- 10 days ahead. To achieve this goal, direct calculation of ET_p by the Penman Monteith equation is used, where weatherforecast is provided by selected NWP model and the prediction of the information of crop status (mainly LAI) are retrieved from VIR-NIR images coupled with a simplified crop growth model. Here we present just the concepts referring to specialized publications for details.

As showed before, in direct calculation, ET_p is estimated by the Penman Monteith equation.
The key features of the procedure are:

- implementation of a crop growth model simulating LAI dynamics;
- application of an ensemble Kalman filter for assimilating LAI from high resolution satellite images within the crop growth model to obtain a stochastic crop model;

- forecasting of metereological data retrieved from NWP (e.g.Cosmo Leps)

A simplified crop growth model with the aim to assess the biomass and LAI growth at daily time step scale is be used (see Fatima Deliverble D.2.2.1). In this class of model the main biophysical processes are conceptualized by a set of simplified analytical relations. A typical approach is the 3PG [52] model where the net primary production (NPP) is modeled according to a light-use efficiency approach with a constant carbon use efficiency factor, similarly to other popular biomass growth models. Other more sophisticated model can be used while maintaining the same approach,

In short, the LAI dynamics is based on temperature and leaf dry matter supply, driven by the development stage of the crop.

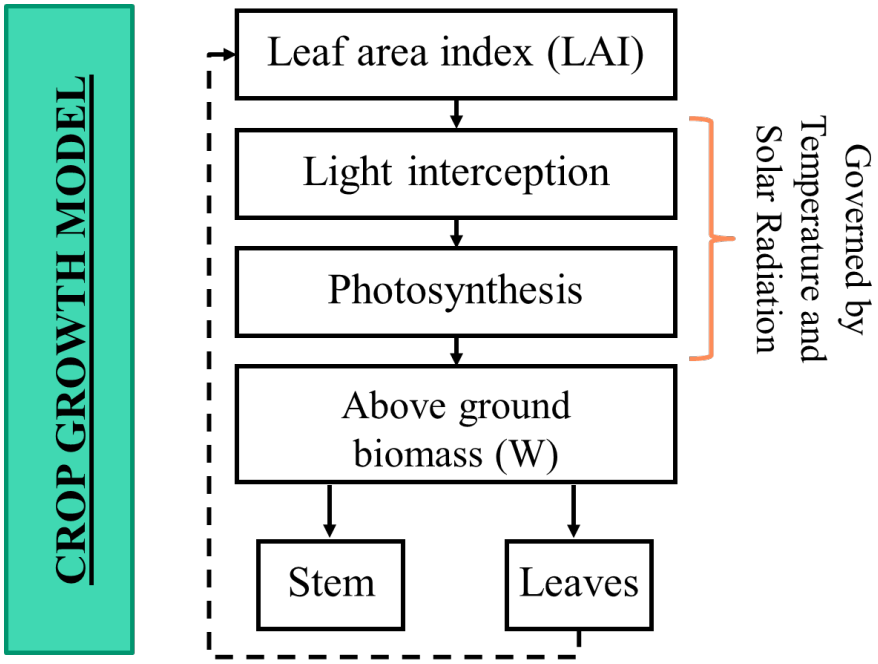

Figure 4.6 - Schema of A simplified crop growth model

Because the crop growth process has inherent errors, including the errors on initial and boundary conditions, the forward simulation of the crop model would result in an increasingly enlarged differences between the simulated and observed results. Remote sensing technology is able to quantitatively depict crop growth conditions and reflect the impact of environmental factors on crop growth and development [53]. Remote sensing information and a crop model can be coupled in different strategies: here the idea is to assimilate LAI measurements by means of an Ensemble Kalman Filter [54], which is a recursive Bayesian ensemble-based filter that estimates the state variable of a dynamic system from a series of noise corrupted measurements, to mitigate modeling uncertainty, i.e. to update model state predictions. In this way the model state variables are continuously updated when remote sensing information is available.

4.9.1 Example of Forecasting Potential evapotranspiration (ETp)

The complete of Penman Monteith formula written in terms of LAI is used.

$$ET_PM = \frac{1}{\lambda}\cdot\frac{\Delta}{\Delta+\gamma^*}\cdot 86400\cdot\left[(1-\alpha)\cdot R_i - |R_{nl}| - \left(0.4\cdot e^{-\frac{LAI}{2}}\cdot R_n\right)\right] + \frac{\gamma}{(\Delta+\gamma^*)}\cdot\frac{0.622\cdot 3.48\cdot 86400}{1.01}\cdot(r_a\cdot U)\cdot\frac{U\cdot(e_a-e_d)}{T+273}$$

(4.1)

To estimate the daily evapotranspiration, meteo data and satellite VIR/NIR images are need.

The 16 terms that COSMO-LEPS model provides for weather's variables are used: 16 evapotranspiration's values are calculated and then performs the media.

The weather's variables are provide from COSMO-LEPS model with GRIB file: Grib is the format used by the meteorological institutes to transport, manipulate and spatialize data meteo.

Lai and Albedo from Satellite Images are interpreted as a step function: they are considered constant until the new acquisition.

Following all calculation steps.

Input GRIB data:

- Temperature Air: T_{avg} [°C] Aggregate to daily scale with average value
- Relative Air Humidity: RH [%] Aggregate to daily scale with average value
- Total Incoming Radiation: R_i [W/m^2] Aggregate to daily scale with sum
- Wind: U [m/s] Aggregate daily scale to with average value
- Atmospheric Pressure: P_a [Pa] Aggregate daily scale to with average value
- Net Longwave Radiation: R_{nl} [W/m^2] Aggregate daily to scale with sum

Input Satellite Images:

- LAI: LAI [m^2/m^2]
- Albedo: α [-]

Parameters:

- Height of Crop: h_c [m]
- cp/e [-] (value assumed=1615)
- ra·U [-]
- rc [m^2/m^2]
- Latitude: Lat [rad]

System of equation to resolve the Penman Monteith formula is the following:

1) ea =0.611·EXP(17.27·Tavg/(Tavg+237.3)) [kPa]
2) ed =RH·ea/100 [kPa]
3) D=4098·ea/((Tavg+237.3)^2) [kPa/°C]
4) l=(2.501-0.002361·Tavg)·1000000 [J/kg]
5) r=3.486·Pa/(Tavg+273) [kg/m^3]
6) g=cp/e·Pa/l [kPa/°C]
7) cp =g·0.622·l/Pa [J/kg/°K]

8) $g^* = g \cdot (1 + rc/(ra \cdot U/U))$ [J/kg/°K]

Where:

- rc = IF (LAI<=4; 200/LAI; 50)
- $ra \cdot U = \ln((2-2 \cdot hc/3)/(0.123 \cdot hc)) \cdot \ln((2-2 \cdot hc/3)/(0.0123 \cdot hc))/0.41^2$
- hc=0.4 [m]
- ln = natural logarithm

9) Rns =(1- α)·Ri [W/m^2]

10) Rn =Rns-|Rnl| [W/m^2]

11) G =0.4·EXP(-0.5·LAI)·Rn [W/m^2]

12) ETrad =(D/(D+g*))·86400·(Rns-|Rnl|-G)/ l [mm/d]

13) ETaero=g/(D+g*)·(0.622·3.486·86400/1.01/ra·U)·U·(ea-ed)/(Tavg+273) [mm/d]

14) ET_p =ETrad+ETaero [mm/d]

15) Fabb_Irr =ET_p-Pn [mm/d]

Where:

- Pn= IF(P>4; (P-4)·0.7; 0)
- Or a version that takes into account the LAI and fcover, according to the following equation:

$$P_n = P - a \cdot LAI \left(1 - \frac{1}{1 + \frac{fcover \cdot P}{a \cdot LAI}} \right)$$

where P is the total rainfall, expressed in cm d^{-1} and a ~0.28 cm d^{-1} for most part of crops.

References

[1] R. Allen, L. S. Pereira, D. Raes, and M. Smith, *Crop evapotranspiration: Guidelines for computing crop requirements*, no. 56. 1998.

[2] G. Hargreaves and Z. Samani, "Reference crop evapotranspiration from ambient air temperature.," *… (Microfiche Collect. no. fiche no …*, 1985.

[3] C. Priestley and R. Taylor, "On the assessment of surface heat flux and evaporation using large-scale parameters," *Mon. Weather Rev.*, 1972.

[4] D. Troufleau, J. P. Lhomme, B. Monteny, and a. Vidal, "Sensible heat flux and radiometric surface temperature over space Sahelian vegetation. I. An experimental analysis of the kB-1 parameter," *J. Hydrol.*, vol. 188–189, pp. 815–838, 1997.

[5] J. Wright, "New evapotranspiration crop coefficients," *… , J. Irrig. Drain. …*, 1982.

[6] H. Braden, "Ein energiehaushalts-und verdunstungsmodell for wasser und stoffhaushaltsuntersuchungen landwirtschaftlich genutzer einzugsgebiete," *Mittelungen Dtsch. Bodenkundliche Geselschaft*, 1985.

[7] M. A. Gilabert, S. Gandía, and J. Meliá, "Analyses of spectral-biophysical relationships for a corn canopy," *Remote Sens. Environ.*, vol. 55, no. 1, pp. 11–20, 1996.

[8] N. Rosenberg, B. Blad, and S. Verma, "Microclimate: the biological environment," 1983.

[9] A. Calera Belmonte, A. M. Jochum, A. Cuesta Garcia, A. Montoro Rodriguez, and P. Lopez Fuster, "Irrigation management from space: Towards user-friendly products," *Irrig. Drain. Syst.*, 2005.

[10] M. Jochum and A. Calera, "Operational Space-Assisted Irrigation Advisory Services: Overview Of And Lessons Learned From The Project DEMETER," *Earth Obs. Veg. …*, 2006.

[11] M. Moran, Y. Inoue, and E. Barnes, "Opportunities and limitations for image-based remote sensing in precision crop management," *Remote Sens. Environ.*, 1997.

[12] W. Bausch and C. Neale, "Crop coefficients derived from reflected canopy radiation: a concept," *Trans. ASAE-American Soc. …*, 1987.

[13] C. Neale, W. Bausch, and D. Heermann, "Development of reflectance-based crop coefficients for

corn," *Trans. ASAE (…*, 1989.

[14] W. C. Bausch, "Soil background effects on reflectance-based crop coefficients for corn," *Remote Sens. Environ.*, vol. 46, no. 2, pp. 213–222, 1993.

[15] J. Gonzalez-Piqueras, A. Calera, M. A. Gilabert, A. Cuesta, and F. D. Tercero, "Estimation of crop coefficients by means of optimized vegetation indices for corn," *Remote Sens. Agric. Ecosyst. Hydrol. V*, vol. 5232, no. 2, pp. 110–118, 2004.

[16] I. Campos, C. Neale, and A. Calera, "Assessing satellite-based basal crop coefficients for irrigated grapes (Vitis vinifera L.)," *Agric. water …*, 2010.

[17] I. Campos, J. Villodre, A. Carrara, and A. Calera, "Remote sensing-based soil water balance to estimate Mediterranean holm oak savanna (dehesa) evapotranspiration under water stress conditions," *J. Hydrol.*, 2013.

[18] E. Rafn, B. Contor, and D. Ames, "Evaluation of a method for estimating irrigated crop-evapotranspiration coefficients from remotely sensed data in Idaho," *J. Irrig. Drain. …*, 2008.

[19] S. Barbagallo, S. Consoli, and A. Russo, "A one-layer satellite surface energy balance for estimating evapotranspiration rates and crop water stress indexes," *Sensors*, 2009.

[20] A. Blanta, D. Nicolas, A. Maliara, and N. Spyropoulos, "Monitoring Cotton Crop Evapotranspiration Based On Satellite Data.," *HAICTA*, 2011.

[21] Joe T. Ritchie, "Model for predicting Evaporationfrom row crop with incomplete cover," *Water Resour. Res.*, vol. 8, no. 5, pp. 1204–1213, 1972.

[22] F. Vuolo, G. D'Urso, C. De Michele, B. Bianchi, and M. Cutting, "Satellite-based irrigation advisory services: A common tool for different experiences from Europe to Australia," *Agric. Water Manag.*, vol. 147, pp. 82–95, 2015.

[23] J. Clevers, "Application of a weighted infrared-red vegetation index for estimating leaf area index by correcting for soil moisture," *Remote Sens. Environ.*, 1989.

[24] S. McLin and L. Gelhar, "field comparison between the USBR-EPA hydrosalinity and generalized lumped parameter models," *Proceedings... Hydrol. areas low …*, 1979.

[25] R. a. Feddes, P. Kabat, P. J. T. Van Bakel, J. J. B. Bronswijk, and J. Halbertsma, "Modelling soil water dynamics in the unsaturated zone — State of the art," *J. Hydrol.*, vol. 100, no. 1–3, pp. 69–111, 1988.

[26] S. Workman and R. Skaggs, "Comparison of two drainage simulation models using field data," *Trans. ASAE*, 1989.

[27] E. Lorre, B. Lesaffre, and R. Skaggs, "Comparison of models for subsurface drainage in flat and sloping lands," *J. Irrig. Drain. …*, 1994.

[28] R. S. Clemente, R. D. Jong, H. N. Hayhoe, W. D. Reynolds, and M. Hares, "Testing and comparison of three unsaturated soil water flow models," *Agric. Water Manag.*, vol. 25, no. 2, pp. 135–152, Apr. 1994.

[29] R. De Faria and C. Madramootoo, "Comparison of the versatile soil moisture budget and SWACROP models for a wheat crop in Brazil," *Can. Agric. …*, 1994.

[30] W. G. M. Bastiaanssen, J. Huygen, J. K. Schakel, and B. J. van den Broek, "Modelling the soil-water-crop-atmosphere system to improve agricultural water management in arid zones (SWATRE)." 1996.

[31] A. Ines, P. Makin, and A. I. Das Gupta, "Crop growth and soil water balance modeling to explore water management options," 2001.

[32] "Following practices, soil water storage, plant-available soil nitrogen accumulation and wheat performance in South West Queensland," *Soil Tillage …*, 1992.

[33] B. Singh and D. Singh, "Agronomic and physiological responses of sorghum, maize and pearl millet to irrigation," *F. Crop. Res.*, 1995.

[34] D. Hillel, "Environmental soil physics: Fundamentals, applications, and environmental considerations," 1998.

[35] R. A. Feddes and H. Zaradny, "Model for simulating soil-water content considering evapotranspiration — Comments," *J. Hydrol.*, vol. 37, no. 3–4, pp. 393–397, May 1978.

[36] J. Dam, J. Huygen, and J. Wesseling, "Theory of SWAP version 2.0; Simulation of water flow, solute transport and plant growth in the Soil-Water-Atmosphere-Plant environment.," 1997.

[37] J. Wesseling and B. Van den Broek, "Prediction of irrigation scheduling with the numerical model SWATRE," *Agric. water Manag.*, 1988.

[38] R. Feddes and W. Bastiaanssen, "Forecasting soil-water-plant-atmosphere interactions in arid regions," *Water Sav. Tech. plant …*, 1992.

[39] S. Elmaloglou and N. Malamos, "Simulation of soil moisture content of a prairie field with SWAP93," *Agric. Water Manag.*, vol. 43, no. 2, pp. 139–149, Mar. 2000.

[40] W. M. Organization, *Guide to Agricultural Meteorological Practices 2010*, no. 134. 2010.

[41] A.C.Lorenc, "Analysis methods for numerical weather prediction," *Royal Meteorological Society*, vol.

112, no. 474. pp. 1177–1194, 1986.

[42] E. N. Lorenz, “The predictability of a flow which possesses many scales of motion,” *Tellus A*, vol. 21, no. 3, pp. 289–307, 1969.

[43] P. Bechtold, M. Köhler, T. Jung, F. Doblas-Reyes, M. Leutbecher, M. J. Rodwell, F. Vitart, and G. Balsamo, “Advances in simulating atmospheric variability with the ECMWF model: From synoptic to decadal time-scales,” *Q. J. R. Meteorol. Soc.*, vol. 134, no. 634, pp. 1337–1351, Jul. 2008.

[44] S. Er-Raki and A. Chehbouni, “Assessment of reference evapotranspiration methods in semi-arid regions: can weather forecast data be used as alternate of ground meteorological parameters?,” *J. Arid …*, 2010.

[45] D. Silva, F. J. Meza, and E. Varas, “Estimating reference evapotranspiration (ETo) using numerical weather forecast data in central Chile,” *J. Hydrol.*, vol. 382, no. 1–4, pp. 64–71, 2010.

[46] D. Tian and C. Martinez, “Forecasting reference evapotranspiration using retrospective forecast analogs in the southeastern United States,” *J. Hydrometeorol.*, 2012.

[47] K. Perera and A. Western, “Forecasting daily reference evapotranspiration for Australia using numerical weather prediction outputs,” *Agric. For. …*, 2014.

[48] H. L. Cloke and F. Pappenberger, “Ensemble flood forecasting: A review,” *J. Hydrol.*, vol. 375, no. 3–4, pp. 613–626, 2009.

[49] D. J. Stensrud, H. E. Brooks, J. Du, M. S. Tracton, and E. Rogers, “Using Ensembles for Short-Range Forecasting,” *Mon. Weather Rev.*, vol. 127, no. 4, pp. 433–446, 1999.

[50] M. Baldauf, A. Seifert, J. Förstner, D. Majewski, M. Raschendorfer, and T. Reinhardt, “Operational Convective-Scale Numerical Weather Prediction with the COSMO Model: Description and Sensitivities,” *Mon. Weather Rev.*, vol. 139, no. 12, pp. 3887–3905, 2011.

[51] P. Unden, L. Rontu, H. Järvinen, and P. Lynch, “HIRLAM-5 scientific documentation,” 2002.

[52] J. J. Landsberg and R. H. Waring, “A generalised model of forest productivity using simplified concepts ofradiation-use efficiency , carbon balance and partltlonlng,” *For. Ecol. Manage.*, vol. 95, pp. 209–228, 1997.

[53] Y. Zhao, S. Chen, and S. Shen, “Assimilating remote sensing information with crop model using Ensemble Kalman Filter for improving LAI monitoring and yield estimation,” *Ecol. Modell.*, vol. 270, pp. 30–42, 2013.

[54] G. Evensen, “Advanced Data Assimilation for Strongly Nonlinear Dynamics,” *Mon. Weather Rev.*, vol. 125, no. 6, pp. 1342–1354, 1997.

[55] Pu, R.; Landry, S. A comparative analysis of high spatial resolution IKONOS and WorldView-2 imagery for mapping urban tree species. Remote Sens. Environ. 2012, 124, 516–533.